Molecular Therapy
Original Article

Weak Agonistic LPS Restores Intestinal Immune Homeostasis

Alex Steimle,[1,4] Lena Michaelis,[1,4] Flaviana Di Lorenzo,[2] Thorsten Kliem,[1] Tobias Münzner,[1] Jan Kevin Maerz,[1] Andrea Schäfer,[1] Anna Lange,[1] Raphael Parusel,[1] Kerstin Gronbach,[1] Kerstin Fuchs,[3] Alba Silipo,[2] Hasan Halit Öz,[1] Bernd J. Pichler,[3] Ingo B. Autenrieth,[1] Antonio Molinaro,[2] and Julia-Stefanie Frick[1]

[1]Institute of Medical Microbiology and Hygiene, University of Tübingen, Tübingen, Germany; [2]Department of Chemical Sciences, University of Naples Federico II, Naples, Italy; [3]Institute of Radiology, Werner Siemens Imaging Center, Department of Preclinical Imaging and Radiopharmacy, University of Tübingen, Tübingen, Germany

Generated by gram-negative bacteria, lipopolysaccharides (LPSs) are one of the most abundant and potent immunomodulatory substances present in the intestinal lumen. Interaction of agonistic LPS with the host myeloid-differentiation-2/Toll-like receptor 4 (MD-2/TLR4) receptor complex results in nuclear factor κB (NF-κB) activation, followed by the robust induction of pro-inflammatory immune responses. Here we have isolated LPS from a common gut commensal, *Bacteroides vulgatus* mpk (BVMPK), which provides only weak agonistic activity. This weak agonistic activity leads to the amelioration of inflammatory immune responses in a mouse model for experimental colitis, and it was in sharp contrast to strong agonists and antagonists. In this context, the administration of BVMPK LPS into mice with severe intestinal inflammation re-established intestinal immune homeostasis within only 2 weeks, resulting in the clearance of all symptoms of inflammation. These inflammation-reducing properties of weak agonistic LPS are grounded in the induction of a special type of endotoxin tolerance via the MD-2/TLR4 receptor complex axis in intestinal lamina propria CD11c$^+$ cells. Thus, weak agonistic LPS represents a promising agent to treat diseases involving pathological overactivation of the intestinal immune system, e.g., in inflammatory bowel diseases.

INTRODUCTION

Inflammatory bowel diseases (IBDs) are characterized by chronic relapsing intestinal inflammation, with Crohn's disease (CD) and ulcerative colitis (UC) being the most frequent and clinically relevant forms of this disease complex.[1] The etiology of IBD is considered to be multifactorial, with genetics,[2] environmental factors,[3] and intestinal microbiota composition[4] contributing to the pathology. Therapy of IBD in humans is currently focused on symptomatic treatment, often by means of immunosuppression.[5] Furthermore, IBD patients require intensive medical intervention, rendering IBD not only a major health care but also a growing economic challenge.[6] This underlies the need for novel, low-priced, and innovative therapeutic approaches.

It is widely accepted that the composition of the intestinal microbiota contributes to the progression and outcome of IBD. However, not only the presence, abundance, or proportion of certain live microbial species account for such microbiota-mediated effects. Indeed, the structure, and consequently the endotoxicity, of lipopolysaccharides (LPSs) from gram-negative bacteria determines the outcome of inflammation in a mouse model for experimental colitis.[7] Furthermore, the composition and variety of the intestinal LPSome strongly impact its inflammation-promoting or homeostasis-preserving properties.[8] This makes LPS an interesting potential drug to target dysregulated intestinal immune responses.

LPS, in its smooth form, consists of three distinct domains: (1) an O-specific polysaccharide (O-chain); (2) a core oligosaccharide (core OS); and (3) the lipid A, which anchors LPS to the outer leaflet of the bacterial cell wall.[9] With its highly conserved overall structure and composition, LPS represents an important microbe-associated molecular pattern (MAMP), playing an essential role for the recognition of bacterial invasion by the host innate immune system[10,11] through recognition by the host myeloid-differentiation-2/Toll-like receptor 4 (MD-2/TLR4) receptor complex. Importantly, the chemical structure of LPS, primarily the detailed composition of lipid A, drastically influences its biological activity, ranging from strong activation of the innate immune system in the case of agonistic LPS to a complete block of immune responses in the case of antagonists.[10,12] This different behavior is reflected in diverse binding modes of such lipid A structures to the MD-2/TLR4 receptor complex.[13]

Given the high amount of endogenous LPS in the gastrointestinal lumen, it is important for the mammalian host to avoid overstimulation of immune cells. Two crucial mechanisms contribute to achieving this aim: (1) a tight intestinal epithelial barrier protecting underlying immune cells in the lamina propria (LP) from luminal LPS, and (2) the induction of endotoxin tolerance.

Received 10 December 2018; accepted 8 July 2019;
https://doi.org/10.1016/j.ymthe.2019.07.007.

[4]These authors contributed equally to this work.

Correspondence: Julia-Stefanie Frick, Institute of Medical Microbiology and Hygiene, University of Tübingen, Elfriede-Aulhorn-Str. 6, 72076 Tübingen, Germany.
E-mail: julia-stefanie.frick@med.uni-tuebingen.de

Endotoxin tolerance denotes a phenotype of antigen-presenting cells that are hyporesponsive toward a second LPS (endotoxin) stimulus through receptor desensitization as the result of a first LPS stimulus.[14,15] Although being a well-documented phenomenon, the molecular mechanisms underlying endotoxin tolerance still remain incompletely understood. Endotoxin tolerance has been observed both *in vitro* and *in vivo* in animal models as well as in humans.[16] The hyporesponsiveness of endotoxin-tolerant cells is reflected in their inability to express and secrete pro-inflammatory cytokines, such as interleukin (IL)-12, IL-6, and IL-1β, in response to a second LPS stimulus.[14] However, the detailed pattern of tolerant genes is cell type dependent.[16] Noteworthy, not only cytokine expression is drastically reduced during endotoxin tolerance but also surface expression of T cell-activating molecules, such as major histocompatibility complex (MHC) class II and CD40.[17,18]

Endotoxin tolerance is established while LPS-stimulated antigen-presenting cells undergo maturation characterized by increased expression of pro-inflammatory cytokines and MHC class II surface expression. So-called semi-mature cells, however, exhibit tolerance toward a secondary LPS stimulus, but they fail to express pro-inflammatory cytokines in response to the first, semi-maturation-inducing stimulus.[19] For example, the well-documented mouse gut commensal *Bacteroides vulgatus* mpk (BVMPK) induces semi-mature $CD11c^+$ cells in the intestinal LP, which is thought to contribute to immunomodulating properties of this bacterial strain, resulting in the prevention of colitis induction in several mouse models for experimental colitis.[20–22] BVMPK belongs to the bacterial phylum *Bacteroidetes*, which represents the most abundant gram-negative phylum in the mammalian gut.[23] Notably, not only BVMPK but also other *Bacteroides* species, such as *Bacteroides fragilis* (BF), provide beneficial and host immune system-modulating properties.[24] In this context, BF is of particular interest since its advantageous properties were demonstrated to be rooted in a structural component: the zwitterionic polysaccharide A (PSA).

Here we demonstrate that BVMPK drastically reduced already established intestinal inflammation in mice, thus leading to a complete healing of damaged intestinal tissue. Intriguingly, this effect was mirrored by using a structural component other than PSA: LPS. BVMPK LPS was found to exhibit weak agonistic activity for interaction with the host MD-2/TLR4 receptor complex, and the administration of purified BVMPK LPS re-established intestinal immune homeostasis in a mouse model for experimental colitis. The weak agonistic properties of this LPS are thought to be responsible for its active amelioration of inflammation through the induction of semi-mature LP $CD11c^+$ cells. Hence, weak agonistic LPS might be a novel and effective therapeutic agent for the treatment of intestinal inflammatory disorders such as IBD.

RESULTS

BVMPK Actively Ameliorates Established Inflammatory Reactions in a Mouse Model for Experimental Colitis, as Confirmed by Non-invasive *In Vivo* PET Imaging

We have already demonstrated that mouse gut-associated commensal BVMPK exhibits anti-inflammatory properties in various different mouse models for experimental colitis.[20–22] These anti-inflammatory properties appeared when BVMPK was administered before the onset of disease, resulting in the prevention of microbiota-mediated intestinal inflammation. This prompted us to verify whether this commensal was also capable of reducing inflammatory reactions in an already inflamed environment. Since we aimed to induce long-term chronic inflammatory conditions, we chose a T cell transplantation model[25] using *Rag1*-deficient mice, which fail to express functional T and B cells.[26] Upon transplantation of naive $CD4^+$ T cells, these $Rag1^{-/-}$ mice develop a chronic form of intestinal inflammation, which is highly dependent on the microbiota composition.[27]

Therefore, we transplanted $Rag1^{-/-}$ mice harboring a highly dysbiotic microbiota (DYSM)[7] with 5×10^5 naive wild-type (WT) $CD4^+CD62L^+CD45Rb^{hi}$ T cells. The composition of the microbiota is described in the Materials and Methods. At 4 weeks after T cell transplantation, mice were administered 5×10^8 viable BVMPK/mL drinking water until the end of the experiment. BVMPK-containing drinking water was renewed every 2 days, and anaerobic BVMPK remained viable under these conditions due to its aerotolerant properties (data not shown). Untreated $Rag1^{-/-}$ mice were used as negative controls, and T cell-transplanted mice that were not administered BVMPK were used as positive controls (Figure 1A).

Since we aimed to real-time monitor the progression of intestinal inflammation in each individual, we injected all mice with [^{18}F]-fluorodeoxyglucose ([^{18}F]FDG), and we performed non-invasive *in vivo* positron emission tomography (PET). [^{18}F]FDG is suitable for the detection of ongoing inflammatory processes in living animals, since sites of inflammation are depicted as regions with higher [^{18}F]FDG uptake in PET scans compared to non-inflamed surrounding environments.[28] However, some organs such as heart and bladder generally provide a basic tracer uptake signal independent of their inflammatory status. We monitored the colonic [^{18}F]FDG uptake over time from all mice used for this experiment. Therefore, each mouse was injected with [^{18}F]FDG, and PET imaging was performed at the day of T cell transplantation (week 0) as well as 4, 6, and 8 weeks after T cell transplantation (Figure 1B). The obtained data were corrected for decay, due to the half-life time of [^{18}F], and normalized to the injected activity per animal.

As demonstrated in the upper panel of Figure 1B, non-transplanted $Rag1^{-/-}$ mice provided low [^{18}F]FDG uptake during the whole observation period, indicating no ongoing inflammatory processes in the colon. In line with previous publications,[7,22] $Rag1^{-/-}$ mice harboring a DYSM and transplanted with naive T cells exhibited severe colonic inflammation, as illustrated by a high colonic [^{18}F]FDG uptake at weeks 4 and 6 (Figure 1B, middle panel). Since the inflammation in these animals exceeded an ethically justifiable level, these animals had to be sacrificed at week 6. As a third group, T cell-transplanted $Rag1^{-/-}$ mice, displaying severe signs of intestinal inflammation at week 4 (Figure 1B, lower panel), were administered viable BVMPK via drinking water from week 4 to week 8 after T cell transplantation. In these mice, we observed a considerable reduction in colonic [^{18}F]

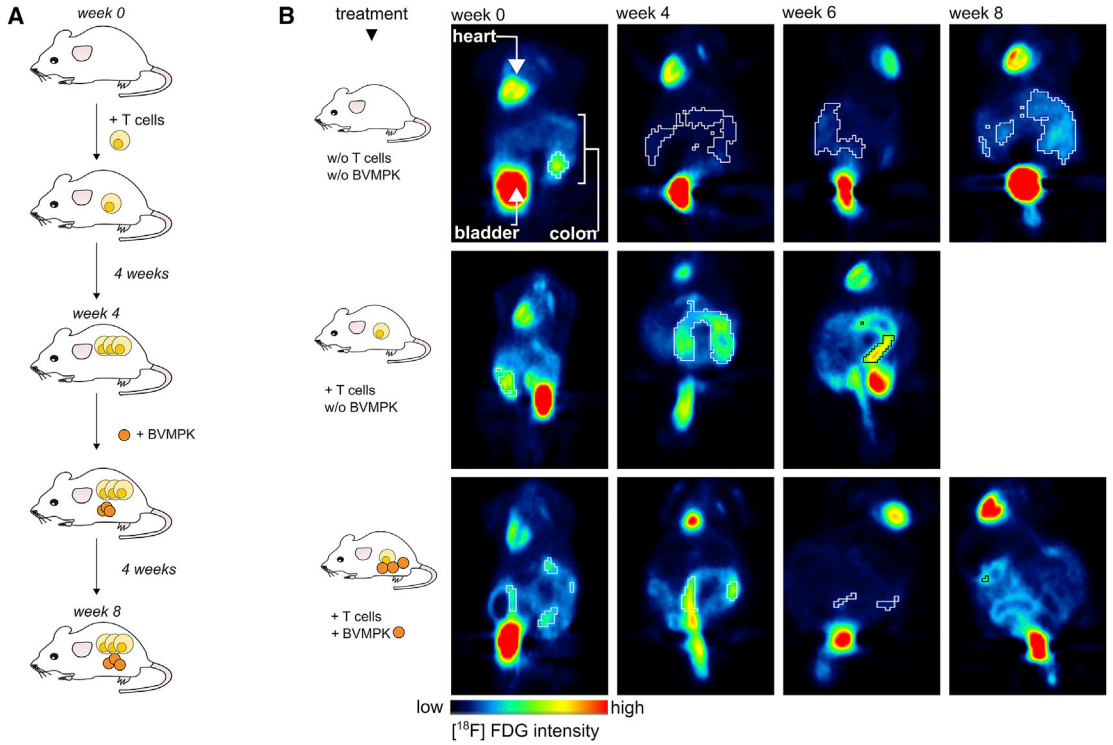

Figure 1. Administration of Live *B. vulgatus* mpk Reduces Intestinal Inflammation in *Rag1*$^{-/-}$ Mice with Established Colonic Inflammation, as Confirmed by Non-invasive *In Vivo* PET Imaging

(A) Experimental setup: *Rag1*$^{-/-}$ mice harboring a highly dysbiotic microbiota were transplanted with CD4^{+} T cells to induce intestinal inflammation as described. 4 weeks after T cell transplantation, mice started receiving live *B. vulgatus* mpk (BVMPK) in the drinking water at a concentration of 5×10^{8} mL^{-1}. BVMPK treatment was continued for 4 more weeks. 8 weeks after T cell transplantation, mice were sacrificed and analyzed. As controls, one group was transplanted without the following BVMPK administration and one group was not T cell transplanted. (B) High-resolution non-invasive small animal *in vivo* PET imaging. 8.3 ± 1.3 MBq [^{18}F]FDG was injected into the tail vein of each mouse. Static PET scans were performed at the day of T cell transplantation and repeated 4, 6, and 8 weeks after T cell transplantation. Data were corrected for decay and normalized to the injected activity. PET images of one representative individual per group are depicted (n = 8–10 mice per group). Organs providing high-intensity signals (heart, bladder, and inflamed colon) are labeled in the upper left panel.

FDG uptake already after 2 weeks. Another PET scan at week 8 revealed comparably low [^{18}F]FDG uptake, indicating that the inflammatory processes, visible at week 4, were cleared by BVMPK administration. The PET results were confirmed by a reduced histological score and a reduced IL-17 expression in BVMPK-fed T cell-transplaned *Rag1*$^{-/-}$ mice, as compared to only T cell-transplaned *Rag1*$^{-/-}$ mice (Figures 4B–4D).

This clearly demonstrated that the anti-inflammatory properties of the commensal BVMPK did not only prevent the induction of inflammation in T cell-transplanted *Rag1*$^{-/-}$ mice, as published previously,[22] but also actively ameliorated already established colonic inflammation, alleviating symptoms of colitis in this mouse model.

Induction of Hyporesponsive CD11c^{+} Cells Is a Common Feature of Various *Bacteroides* Species

We have already demonstrated that BVMPK-mediated suppression of intestinal inflammation strongly correlates with the induction of a hyporesponsive or so-called semi-mature phenotype of LP CD11c^{+} cells.[7,22] We assumed that such hyporesponsive LP CD11c^{+} cells were responsible for the observed inflammation-preventing and -reducing effects in *in vivo* models for experimental colitis. Since *Bacteroidetes* represents the major gram-negative phylum in the human intestine,[29,30] we aimed to examine the semi-maturation-inducing properties of *Bacteroides* species other than BVMPK, namely, *B. dorei* (BD), *B. vulgatus* ATCC8482 (BV8482), BF, and *B. thetaiotaomicron* (BTIO).

It was already demonstrated that BVMPK induced semi-maturation *in vitro* in bone marrow-derived dendritic cells (BMDCs). This phenotype is characterized by low but measurable secretion of IL-6 with the simultaneous absence of secretion of other pro-inflammatory cytokines, such as tumor necrosis factor (TNF), IL-12, and IL-1β, as well as the absence of anti-inflammatory IL-10.[22,31] Furthermore, semi-mature BMDCs (smBMDCs) only provide slightly increased surface expression of MHC class II, CD40, CD80, and CD86.[22,31] In general, LP CD11c^{+} cells strongly resemble BMDCs, as shown by comparable expressions of CD45, CD11b, and CD103 while being CD3neg, Ly6Gneg, Ly6Gneg, CD45Rneg, and CD64neg (Figure S1). Therefore, we used BMDCs to assess whether *Bacteroides* strains

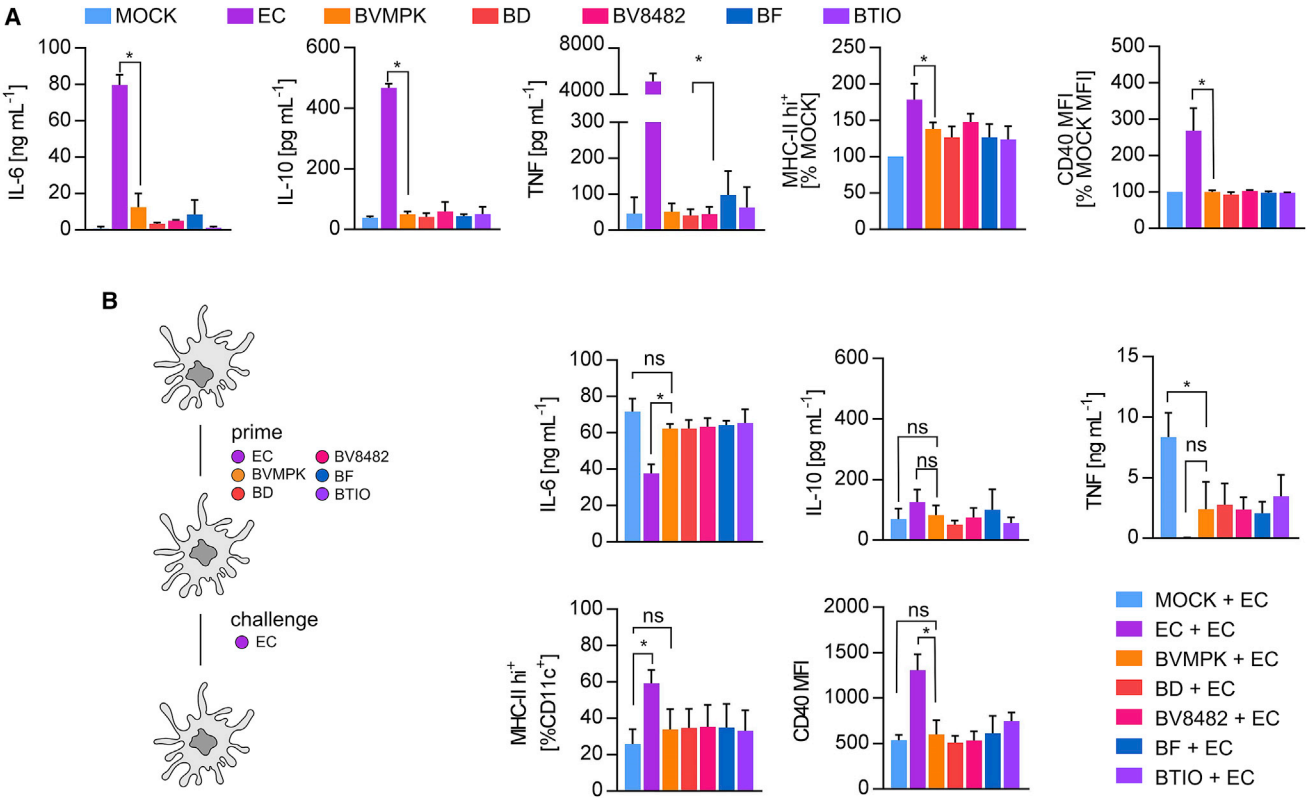

Figure 2. Induction of Hyporesponsive CD11c$^+$ Cells Is a Common Feature of Various *Bacteroides* Species

(A) Stimulation of CD11c$^+$ bone marrow-derived dendritic cells (BMDCs) generated from WT C57BL/6 mice (n = 3 mice) with PBS (mock), *E. coli* mpk (EC), *B. vulgatus mpk* (BVMPK), *B. dorei* (BD), *B. vulgatus* ATCC8482 (BV8482), *B. fragilis* (BF), and *B. thetaiotaomicron* (BTIO) for 16 h at an MOI of 1. Cytokine secretion was detected by ELISA. Surface expressions of MHC class II and CD40 were detected by flow cytometry, and the population of MHC class II hi$^+$ cells and CD40 MFI, respectively, were normalized to the mock control of BMDCs generated from the same individual. (B) WT BMDCs (n = 3 mice) were stimulated with PBS (mock), EC, BVMPK, BD, BV8482, BF, and BTIO at an MOI of 1 for 24 h (prime). Cell culture medium was removed and exchanged for fresh medium before stimulation (challenge) with EC for an additional 16 h. Cytokine secretion was detected by ELISA. Surface expressions of MHC class II and CD40 were detected by flow cytometry. Statistical analysis was performed using one-way ANOVA. p values <0.05 were considered to be statistically significant and are indicated with an asterisk (*). Columns and error bars represent mean ± SD.

other than BVMPK induce the effects of hyporesponsiveness in CD11c$^+$ cells.

BMDCs were generated from the bone marrow of WT C57BL/6N mice, and they were stimulated for 16 h with PBS (mock) as a negative control as well as with BVMPK, BD, BF, BV8482, and BTIO. *E. coli* mpk (EC) was used as a positive control to induce fully mature BMDCs.[22] All bacteria were added to BMDCs at an MOI of 1. As demonstrated by the low secretion of IL-6, the absence of IL-10 and TNF, as well as by only slightly increased MHC class II and CD40 surface expressions, all tested *Bacteroides* strains induced comparable effects in BMDCs, which were comparable to BVMPK-induced effects, therefore suggesting the induction of semi-maturation by all tested *Bacteroides* strains (Figures 2A and S2). As expected, EC stimulation led to the strong secretions of IL-6, IL-10, and TNF as well as increased MHC class II and CD40 surface levels.

A characteristic feature of BVMPK-induced semi-mature (sm) CD11c$^+$ cells is hyporesponsiveness toward further bacterial stimuli in terms of surface expressions of MHC class II, CD40, CD80, and CD86 as well as secretions of cytokines, such as TNF, but not IL-6. Therefore, we primed BMDCs with BVMPK, BD, BV8482, BF, BTIO, or EC for 24 h and challenged them with EC. Importantly, medium was changed between prime and challenge to determine whether primed cells were still capable of secreting pro-inflammatory cytokines in response to EC challenge. As seen in Figure 2B, IL-6 secretion was not reduced in *Bacteroides*-primed and EC-challenged BMDCs compared to unprimed EC-challenged BMDCs. IL-10 secretion was generally low among all different stimulus combinations. However, priming of BMDCs with all tested *Bacteroides* strains resulted in the tolerance of TNF expression after EC challenge in contrast to unprimed BMDCs. In line with this, priming of BMDCs with all tested *Bacteroides* strains resulted in (significantly) lower MHC class II and CD40 surface expressions after EC challenge compared to EC-primed BMDCs. However, these results point at the induction of semi-maturation and, therefore, tolerance toward TNF and surface T cell-activating surface molecule expression by all tested *Bacteroides* species. Thus, the induction of smBMDCs is not a unique property of BVMPK.

Table 1. Comparison of the Lipid A Core Synthesis Genes between BVMPK and BV8482, BD, and BTIO

BVMPK	BV8482		BD		BTIO	
ID	ID	SIM (%)	ID	SIM (%)	ID	SIM (%)
BvMPK_3283	BVU_0099	100	HMPREF1064_02220	99	BT4205	82
BvMPK_3832	BVU_0098	99	HMPREF1064_02221	99	BT4206	86
BvMPK_3821	BVU_0097	99	HMPREF1064_02222	99	BT4207	69
BvMPK_4264	BVU_0525	100	HMPREF1064_04085	99	BT3697	84
BvMPK_1137	BVU_1917	99	HMPREF1064_04942	97	BT4004	74
BvMPK_0444	BVU_1603	99	HMPREF1064_03036	96	BT1880	100
BvMPK_1465	BVU_1476	99	HMPREF1064_03097	98	BT2747	66
BvMPK_0774	BVU_1062	98	HMPREF1064_01726	97	BT2152	34
BvMPK_3353	BVU_3834	99	HMPREF1064_04014	96	not identified	
BvMPK_0983	BVU_1238	99	HMPREF1064_01498	93	not identified	
BvMPK_2934	BVU_3293	99	HMPREF1064_03350	98	BT1854	48

Genetic similarities (SIMs) were calculated by alignment of the genes from BV8482, BD, and BTIO compared to BVMPK. IDs refer to the respective gene identifiers.

Bacteroides Species Share a Conserved Lipid A Synthesis Core

Since stimulation with heat-killed BVMPK, BD, BF, BV8482, and BTIO also resulted in BMDC semi-maturation as induced by viable bacteria (see also Figure S3), we supposed the crucial semi-maturation-inducing bacterial factor to be a structural component that is shared by all these strains. *Bacteroides* belong to gram-negative bacteria and harbor LPS in the outer membrane of the bacterial cell wall. LPS is known to be one of the most potent surface molecules and dendritic cell (DC) maturation-inducing components of gram-negative bacteria. It consists of lipid A, a core oligosaccharide, and an O-antigen composed of polysaccharides of various lengths. Jacobson et al.[32] have recently reported on the differences in the poly- and oligosaccharide portions among BF, BV8482, BD, and BTIO. Since all these strains induced semi-maturation in our experiments (Figure 2), we hypothesized that the induction of semi-maturation occurs independently of LPS carbohydrate moieties. Therefore, we focused on the lipid A part. Lipid A of BD and BF was reported to be similar in structure and composition, being mono-phosphorylated and harboring only 5 acyl chains.[33,34]

To identify candidate genes for *Bacteroides* lipid A biosynthesis, we performed BLASTP searches against genomes of BV8482, BD, and BTIO using BVMPK genes as reference. We found lipid A biosynthesis genes of all investigated *Bacteroides* spp. to be homologous, since, with some exceptions for BTIO, the similarities among the sequences exceeded 90% (Table 1). In the next step, we compared the biosynthesis genes for BVMPK lipid A with the Raetz pathway of EC (Table 2). We could clearly show that *Bacteroides* lipid A synthesis genes differ significantly from the EC lipid A synthesis genes. The similarities between the genes were only between 25% and 42%, and the EC genome was found to lack the BVMPK_0774 and BVMPK_3353 (Table 2). These differences probably result in different lipid A compositions. The observed gene homology among the lipid A cores of BVMPK, BD, BTIO, and BV8482 is in line with our hypothesis that immunogenic effects on dendritic cells by all tested *Bacteroides* spp. are mediated by their typical LPS. Correspondingly, EC, which produces a different type of LPS, induced clearly different effects. Overall, this suggests that the structure of *Bacteroides* spp. LPS is a crucial determinant for the induction of semi-maturation in $CD11c^+$ cells. Work is ongoing to establish the chemical structure of LPS from BVMPK (LPSBV) and its structure-activity relationship.

Isolated LPS of BVMPK Induces Hyporesponsive Semi-mature $CD11c^+$ Cells

To verify the hypothesis that *Bacteroides* spp. LPS is crucial for the induction of hyporesponsive $CD11c^+$ cells, we isolated LPSBV as well as from EC (LPSEC), which contains a strongly agonistic *bis*-phosphorylated and hexaacylated lipid A. We generated BMDCs from WT C57BL/6 mice, and we stimulated these cells with either viable BVMPK or EC at an MOI of 1. Additionally, BMDCs were stimulated with purified LPSBV or LPSEC, both at concentrations of 50 $ng^{-1}/10^6$ BMDCs for a total of 16 h. As shown in Figure 3A, stimulation of BMDCs with LPS resulted in the same BMDC phenotype as stimulation with the respective bacteria from which the LPS was isolated. Both, BVMPK and LPSBV stimulation led to low expressions of MHC class II, CD40, CD80, and CD86 (Figure 3A) as well as to a low secretion of IL-6 and an absence of TNF (Figure 3A). On the contrary, stimulation of BMDCs with either EC or LPSEC led to significant increases in the surface expressions of MHC class II and T cell co-stimulatory molecules CD40, CD80, and CD86 as well as to increased secretions of IL-6 and TNF (Figure 3A).

To assess hyporesponsiveness toward a secondary stimulus, we stimulated BMDCs for 24 h with PBS (mock), BVMPK, LPSBV, EC, and LPSEC followed by a challenge with either EC or PBS as a negative control. Importantly, medium was changed between prime and challenge to determine whether primed cells were still capable of secreting pro-inflammatory cytokines in response to EC challenge. To determine the change in the surface expressions of T cell co-stimulatory molecules in response to EC challenge, we determined the proportion

Table 2. Comparison of the Lipid A Core Synthesis Genes between BVMPK and EC MG1655

BVMPK	EC MG1655	
ID	ID	SIM
BvMPK_3283	944849	42
BvMPK_3832	944816	36
BvMPK_3821	944882	33
BvMPK_4264	949053	27
BvMPK_1137	944838	31
BvMPK_0444	945526	25
BvMPK_1465	949048	26
BvMPK_0774	not identified	
BvMPK_3353	not identified	
BvMPK_0983	945863	35
BvMPK_2934	945450	27

Genetic similarities (SIMs) were calculated by alignment of the genes from *Escherchia coli* K12 MG1655 (EC MG1655) compared to BVMPK. IDs refer to the respective gene identifiers.

of MHC class IIhi$^+$, CD40$^+$, CD80$^+$, and CD86$^+$ cells in primed and EC-challenged BMDCs, and we compared them with PBS-challenged controls that were primed with the same stimulus. Thus, high bars indicate high responsiveness and low bars indicate tolerance (Figure 3B). As demonstrated in Figure 3B, both, BVMPK- and LPSBV-primed EC-challenged BMDCs provided significantly lower secretion of TNF. Furthermore, increases in CD80 and CD86 surface expressions in LPSBV-primed and EC-challenged BMDCs were significantly lower compared to PBS-primed and EC-challenged BMDCs, indicating the induction of hyporesponsiveness of LPSBV-primed cells concerning the surface expressions of T cell-activating molecules. As expected, priming with EC and LPSEC leads to full DC maturation.

To verify that LPSBV- and BVMPK-induced semi-maturating effects on BMDCs are rooted in LPS-dependent TLR4 signaling, we pre-incubated BMDCs for 1 h with the competitive TLR4 antagonist TAK242 (Figure S4) before stimulation with LPSBV, BVMPK, and EC for 16 h (Figure 3C). TAK242 pre-incubation abolished cytokine secretion and modulation of MHC class II and CD40 surface expressions for all the used stimuli. Therefore, we concluded that (1) BVMPK induces BMDC semi-maturation mainly via its LPS, and (2) purified LPSBV is sufficient to induce hyporesponsive semi-mature BMDCs.

TAK242 is described to be a selective TLR4 antagonist,[35,36] and our control experiments confirmed that TAK242 led to an inhibition of TLR4, but not TLR2, signaling. However, we cannot exclude that TAK242 may also influence other signaling pathways.

LPS-mediated induction of TLR4 signaling results in the activation of nuclear factor κB (NF-κB) and, therefore, in the expression of pro- and anti-inflammatory cytokines. Since BVMPK and EC as well as LPSBV induce a different cytokine secretion pattern via TLR4 signaling, we compared the NF-κB-activating potential of BVMPK and EC, as well as of LPSBV and LPSEC. For this purpose, we used HEK cells expressing the mouse MD-2/TLR4 receptor complex (mTLR4-HEK) (Figure 3D), and we stimulated them for 16 h. The resulting IL-8 secretion was detected as an indirect measure of MD-2/TLR4-mediated NF-κB activation, since IL-8 secretion is a direct consequence of TLR4-mediated NF-κB activation.[37] Stimulation of mTLR4-HEK cells with either viable BVMPK or EC at an MOI of 1 resulted in significantly higher IL-8 secretion from EC-stimulated cells compared to BVMPK-stimulated cells (Figure 3D, upper panel). Stimulation of mTLR4-HEK cells with isolated LPSBV or LPSEC resulted in a concentration-dependent increase in IL-8 secretion when LPSBV was used. LPSEC stimulation resulted in saturated IL-8 secretion, even at concentrations as low as 1 ng mL^{-1} (Figure 3D, lower panel). The increased IL-8 secretion as a result of NF-κB activation[37] indicated significantly stronger activation of LPSEC compared to LPSBV in mTLR4-HEK cells. Additionally, we measured the phosphorylation of S534 of the NF-κB subunit p65 (p-p65) via flow cytometry as a measure of NF-κB transactivation activity[38,39] in mouse BMDCs, in response to either LPSBV or viable BVMPK and EC, respectively. Stimulation with BVMPK and LPSBV of BMDCs for 30 min resulted in a significantly lower p-p65 induction compared to EC stimulation (Figure 3E).

Furthermore, we determined intracellular aldehyde dehydrogenase (ALDH) activity in mouse BMDCs stimulated with viable BVMPK or EC for 16 h (Figures 3F and S5). ALDH triggers the induction of inflammation-ameliorating Foxp3$^+$ regulatory T cells (Tregs) by metabolizing vitamin A-derived retinol into retinoic acid (RA).[40] RA has been shown to be a crucial mediator for the induction of Tregs, and ALDH$^+$ intestinal dendritic cells are considered to be important mediators for immune homeostasis.[19,41,42] BVMPK-stimulated BMDCs showed a significantly higher ALDH activity compared to EC-stimulated BMDCs, indicating a stronger Treg induction potential.

LPS is known to be a strong agonist for the MD-2/TLR4 receptor complex. However, it was reported that certain LPS structures also induce TLR2-mediated signaling, i.e., *Helicobacter pylori* LPS,[43] while the TLR2-activating capacity of *Porphyromonas gingivalis* LPS remains controversial and is probably an experimental artifact due to a lipoprotein contamination.[44] Therefore, these reports raise the question for a contribution of TLR2 signaling to the LPSBV-mediated immunogenic effects on CD11c$^+$ cells as well as for a potential contamination of the used LPSBV preparations, which might, in consequence, induce TLR2 receptor activation. Concerning potential and yet unrecognized contaminations, not only lipoproteins but also the presence of capsular polysaccharides has to be considered. During the purification process, an additional ultracentrifugation step was performed to eliminate the presence of capsular polysaccharides from the LPSBV preparations. Nevertheless, we checked whether solubilized LPSBV preparations induce TLR2 signaling, since both

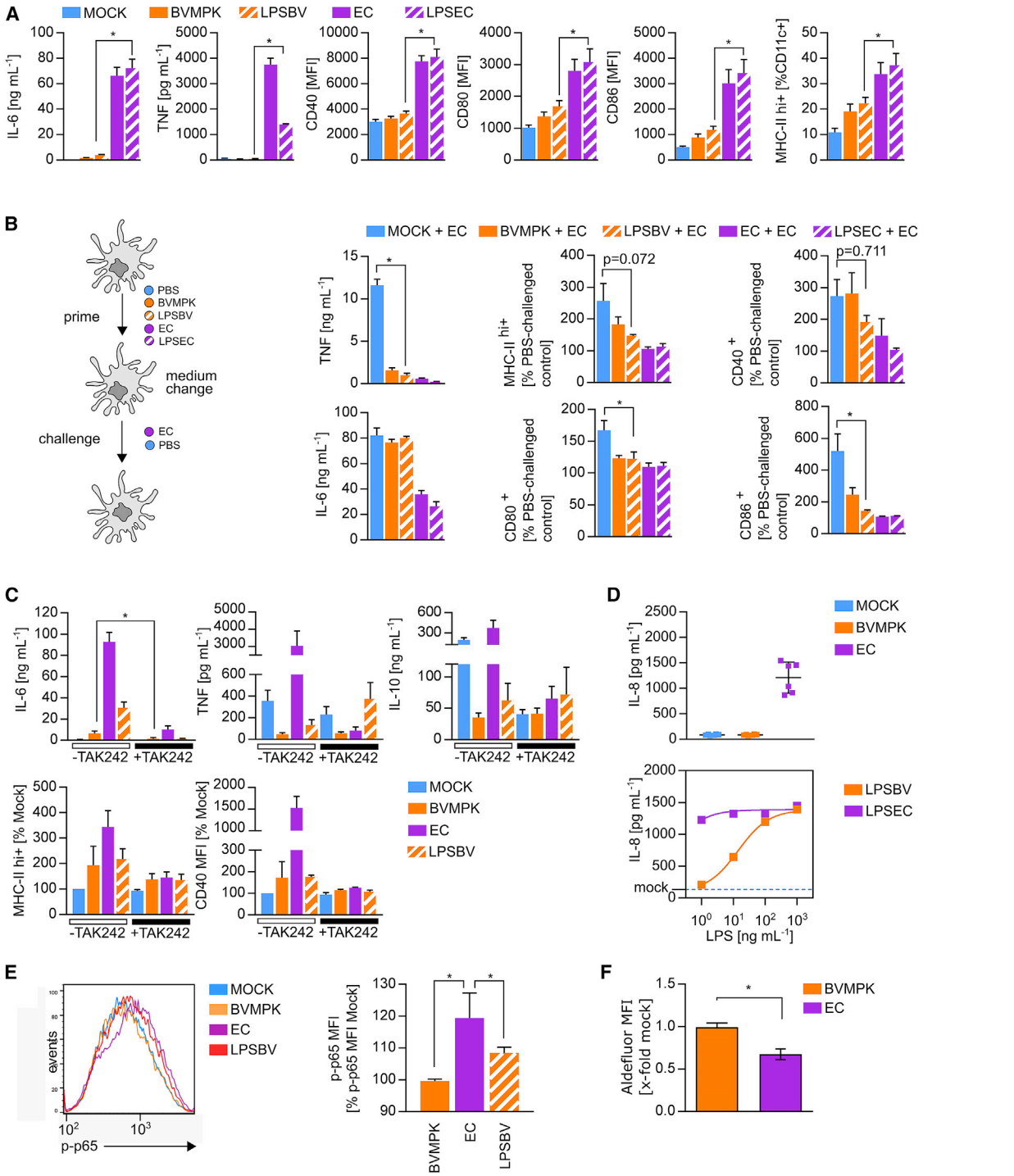

Figure 3. Isolated LPS of BVMPK Induces Hyporesponsive Semi-mature CD11c$^+$ Cells

(A) Stimulation of CD11c$^+$ bone marrow-derived dendritic cells (BMDCs) generated from WT C57BL/6 mice (n = 4 mice) with PBS (mock), *E. coli* mpk (EC), *B. vulgatus mpk* (BVMPK), *E. coli* mpk LPS (LPSEC), and *B. vulgatus* mpk LPS (LPSBV). Cytokine secretion was detected by ELISA. Surface expressions of CD40, CD80, CD86, and MHC class II were detected by flow cytometry. (B) WT BMDCs (n = 4 mice) were stimulated with PBS (mock), EC, LPSEC, BVMPK, and LPSBV for 24 h (prime). Cell culture medium was removed and exchanged for fresh medium before stimulation (challenge) with EC for an additional 16 h. Cytokine secretion was detected by ELISA. Surface expressions of MHC class II, CD40, CD80, and CD86 were detected by flow cytometry, and the population of MHC class II hi$^+$ cells and CD40 MFI, CD80 MFI, and CD86 MFI were normalized to the PBS-challenged control of BMDCs generated from the same individual with the same priming stimulus. (C) Stimulation of CD11c$^+$ bone marrow-derived

(legend continued on next page)

potential contaminants, capsular polysaccharides[45–48] and lipoproteins[49–51] from gram-negative bacteria, would result in TLR2 receptor activation (Figure S6). We detected minor differences in IL-6 secretion of LPSBV-stimulated WT BMDCs compared to TLR2-deficient BMDCs, indicating a slight activation of TLR2 by LPSBV (Figure S6A). However, using *TLR2*$^{-/-}$ BMDCs, we could exclude the contribution of TLR2-mediated signaling to the induction of hyporesponsive semi-mature BMDCs (Figure S6B). Therefore, we conclude that LPSBV-induced MD-2/TLR4 receptor signaling, but not TLR2 signaling, is crucial for the induction of BMDC semi-maturation.

Taken together, these results indicate a significantly weaker MD-2/TLR4 receptor activation of LPSBV compared to LPSEC, resulting in reduced NF-κB transactivation capacity. However, and in contrast to being a MD-2/TLR4 antagonist, LPSBV actively induced hyporesponsive semi-maturation in BMDCs without inducing the expression of pro-inflammatory cytokines. Thus, we suppose LPSBV to be rather weak agonistic than antagonistic.

Administration of Purified LPSBV Reduces Established Intestinal Inflammation in a Mouse Model of Experimental Colitis

Since (1) weak agonistic LPSBV provided the same semi-maturation-inducing capacities as viable BVMPK in BMDCs and (2) BVMPK-mediated prevention of intestinal inflammation in *Rag1*$^{-/-}$ mice correlated with the induction of semi-mature LP CD11c^{+} cells, we were interested to know if the administration of LPSBV resulted in the same inflammation-reducing effects in T cell-transplanted *Rag1*$^{-/-}$ mice. Therefore, we used *Rag1*$^{-/-}$ mice harboring a highly DYSM, and we induced colonic inflammation through the transplantation of 5×10^5 naive WT CD4^{+}CD62L^{+}CD45RB^{hi} T cells. At week 4, transplanted mice showed clear signs of colonic inflammation, such as bloody feces and diarrhea, which is in line with the PET imaging that was performed to monitor intestinal inflammation (Figure 1B). At this point, we started to administer viable BVMPK (5×10^8 bacteria/mL drinking water) as well as LPSBV at a concentration of 160 μg mL^{-1} in the drinking water for 4 additional weeks (Figure 4A). Mice with a C57BL/6 genetic background, such as *Rag1*$^{-/-}$, were reported to consume around 6 mL drinking water each day,[52] suggesting the daily uptake of LPSBV to be around 1 mg/mouse.

Figure 4B illustrates representative H&E-stained colonic sections from each group taken at the end of the experiment. As expected, non-treated T cell-transplanted animals showed severe signs of colonic inflammation (Figure 4B, left panel). However, the LPSBV- and BVMPK-treated animals exhibited significantly lower intestinal inflammation (Figure 4B, middle and right panels) compared to non-treated mice (Figure 4C). CD3^{+}CD4^{+} T cells isolated from the colonic LP (cLP) of live BVMPK-treated *Rag1*$^{-/-}$ mice expressed significantly lower amounts of IL-17 (Figure 4D), thus providing a clearly reduced Th17 response,[53] which crucially contributes to the induction of colitis in this mouse model.

Furthermore, qRT-PCRs from colonic scrapings revealed that live BVMPK-treated animals expressed significantly higher amounts of ALDH mRNA (Figure 4E), which supports our *in vitro* findings of a higher Treg-inducing potential of antigen-presenting cells that encountered BVMPK (Figure 3F).

LPSBV-treated T cell-transplanted *Rag1*$^{-/-}$ mice also provided significantly lower proportions of IL-17-expressing CD3^{+}CD4^{+} cLP T cells as well as higher *Aldh* mRNA expression in colonic scrapings. These data indicated that both live BVMPK and isolated LPSBV are equally able to ameliorate established inflammatory processes in the large intestine, by downregulating the Th17 immune response promoting cytokines and by favoring Treg-inducing environmental conditions.

Weak Agonistic LPSBV Is Not a Competitive Inhibitor of Strong Agonistic LPS

The results obtained from *in vivo* experiments using *Rag1*$^{-/-}$ mice raised the question of whether LPSBV acts as a competitive inhibitor at the MD-2/TLR4 receptor complex-binding site, therefore preventing agonistic LPS from binding and thus inducing complete CD11c^{+} cell maturation characterized by pro-inflammatory immune responses. First, we aimed to determine and compare binding constants of LPSBV and the prototype agonistic LPSEC to the mouse MD-2/TLR4 receptor complex. Therefore, we established an optical titration setting to trigger *quasi* dissociation constants (K_D) of both LPSBV and LPSEC, using biotinylated LPSBV (bioLPSBV). Prior to that, bioLPSBV was confirmed to provide the identical activation of the mouse MD-2/TLR4 receptor complex (Figure S7), therefore suggesting that biotinylation did not affect LPSBV-binding behavior.

We are aware of the fact that we could not determine real K_D values, since we did not know the exact molarity of the used LPS solutions. The assembly of amphiphilic LPS monomers into micelles, vesicles,

dendritic cells (BMDCs) generated from WT C57BL/6 mice (n = 5 mice) with PBS (mock), BVMPK, EC, and LPSBV either with or without pre-incubation with TLR4 receptor antagonist TAK242 at 1 h prior to bacterial stimulation. Cytokine secretion was detected by ELISA. Surface expressions of MHC class II and CD40 were detected by flow cytometry, and the population of MHC class II hi^{+} cells and CD40 MFI, respectively, were normalized to the untreated mock control of BMDCs generated from the same individual. (D) Stimulation of mouse MD-2/TLR4 receptor complex expressing HEK cells (mTLR4-HEK) with PBS (mock), EC, and BVMPK at an MOI of 1 (n = 2 experimental replications with 3 technical replicates, upper panel) or LPSEC and LPSBV at various concentrations (n = 3 technical replicates, lower panel). The resulting IL-8 secretion as a measure of NF-κB activation was detected by ELISA, and it is indicated by a blue line for mock samples in the lower panel. (E) Stimulation of BMDCs (n = 4 mice) with PBS (mock), EC, BVMPK, and LPSBV for 30 min. The resulting phosphorylation of intracellular p65, phosphorylated at S534 (p-p65), was detected by flow cytometry. The resulting MFI was normalized to the mock control of BMDCs generated from the same individual. (F) Stimulation of WT BMDCs (n = 5 mice) with PBS (mock), BVMPK, and EC at an MOI of 1 for 16 h. ALDH levels in BMDCs were then detected using an Aldefluor ALDH activity assay. Statistical analysis was performed using one-way ANOVA (A, B, and E) or Student's t test (C and F). p values <0.05 were considered to be statistically significant and are indicated with an asterisk (*). Columns and error bars represent mean ± SD.

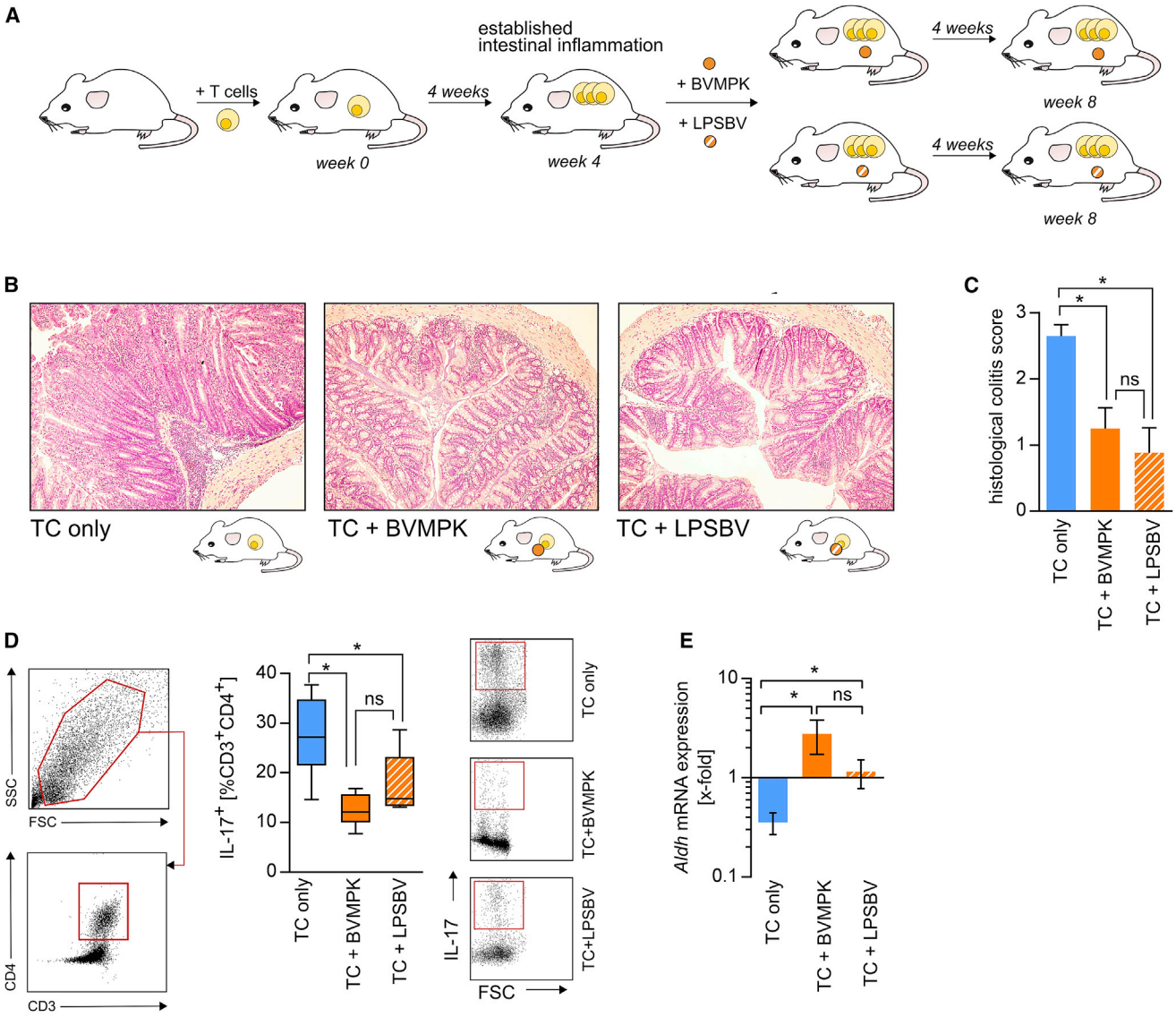

Figure 4. Isolated *B. vulgatus* mpk LPS Provides the Same Capability to Reduce Intestinal Inflammation in *Rag1*$^{-/-}$ Mice with Established Colonic Inflammation as Live *B. vulgatus* mpk

(A) Experimental setup: *Rag1*$^{-/-}$ mice harboring a highly dysbiotic microbiota were transplanted with naive CD4$^+$ T cells to induce intestinal inflammation as described. 4 weeks after T cell transplantation, mice were not treated (TC only, n = 5), treated with live *B. vulgatus* mpk (TC + BVMPK, n = 8) by administration of 5 × 10^8 bacteria mL^{-1} in the drinking water, or treated with isolated *B. vulgatus* mpk LPS (TC + LPSBV, n = 8) in the drinking water at a concentration of 160 μg mL^{-1}. Mice were sacrificed and analyzed 8 weeks after T cell transplantation. (B) Representative H&E-stained colonic sections at week 8. (C) Histological colitis score at week 8, ranging from 0 to a maximum of 3. (D) Left panel: gating strategy to determine the CD3$^+$CD4$^+$ T cell population in the colonic lamina propria (cLP) at week 8. Right panel: proportion of IL-17$^+$ cells among the population of cLP CD3$^+$CD4$^+$ T cells, determined by flow cytometry. (E) Relative *Aldh2* mRNA expression in colonic scrapings at week 8, determined by qRT-PCR. Data were normalized to *Aldh2* mRNA expression in colonic scrapings of non-inflamed non-T cell-transplanted *Rag1*$^{-/-}$ mice. Statistical analysis was performed using Kruskal-Wallis test (C) or one-way ANOVA (D and E). p values <0.05 were considered to be statistically significant and are indicated with an asterisk (*). Columns and error bars represent mean ± SD (C and E). Boxplots depict the mean as well as the 25th and 75th percentiles, and whiskers depict the highest and lowest values (D).

or even more complicated structures is highly dependent on the buffer and ionic strength, and it is, therefore, hardly predictable. This exacerbated the determination of the molarity of LPS monomers, which effectively have access to the receptor, rendering them active ligands thus contributing to K_D values. However, assuming that (1) bioLPSBV and LPSEC provide a comparable monomeric molecular weight, (2) bioLPSBV and LPSEC behave in a similar chemical manner under the experimental conditions, and (3) all experiments were carried out incubating both LPSs at the same time, we can speculate that a qualitative comparison using K_D values in the unit g L^{-1}

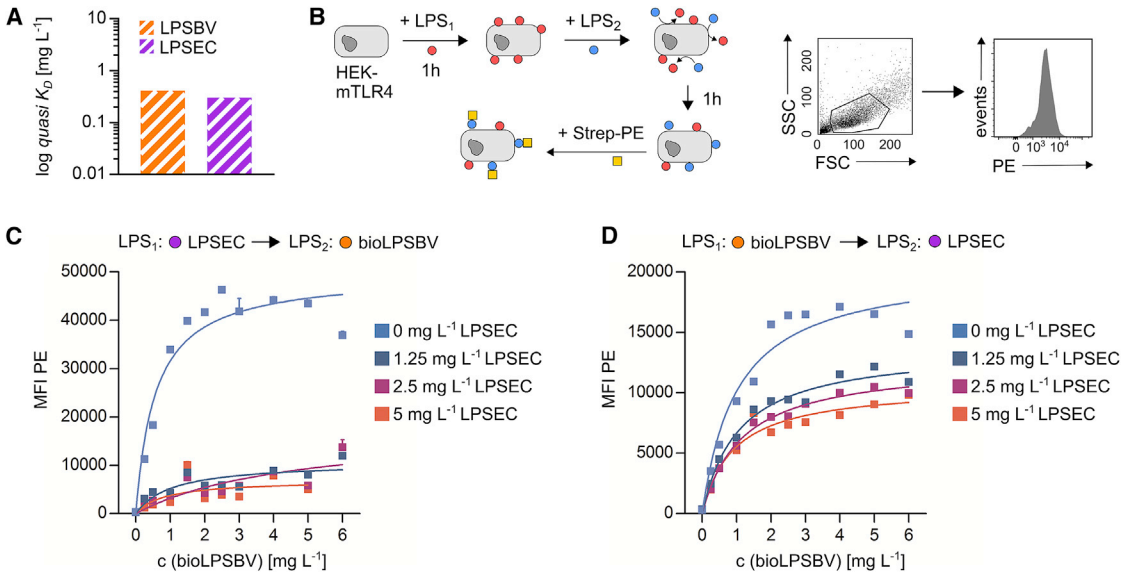

Figure 5. Weak Agonistic LPSBV Is Not a Competitive Inhibitor of Strong Agonistic LPS

(A) Determination of the dissociation constant (g L^{-1}, quasi K_D) of LPSBV and LPSEC using an optical titration-based approach. (B) Left panel: experimental setting. 1×10^5 HEK cells expressing murine CD14, MD-2, and TLR4 (mTLR4-HEK) were incubated with a certain concentration of either LPSEC ranging from 0 to 5 mg L^{-1} or biotinylated LPSBV (bioLPSBV) ranging from 0 to 6 mg L^{-1} for 1 h. After 1 h, the opposite LPS (either LPSBV or LPSEC) was added for an additional 1 h. PE-coupled streptavidin (Strep-PE) was added for 30 min, and the resulting PE fluorescence associated with mTLR4-HEK cells was detected by flow cytometry. Right panel: gating strategy to determine PE fluorescence of intact mTLR4-HEK cells is shown. (C) Binding curves of 4 distinct concentrations of LPSEC added first to mTLR4-HEK (n = 3 technical replicates) plotted against varying concentrations of subsequently added bioLPSBV. (D) Binding curves of 7 distinct concentrations of bioLPSBV added first to mTLR4-HEK (n = 3 technical replicates) plotted against varying concentrations of subsequently added LPSEC. Squares with error bars represent mean ± SD (C and D).

instead of mol L^{-1} is qualifiable for a comparison of their binding affinity. We finally determined quasi K_D to be 0.412 g L^{-1} for LPSBV and 0.304 g L^{-1} for LPSEC (Figure 5A, see also Figure S8 for more details on optical titration). These data allowed us to conclude that LPSBV and LPSEC provide similar binding affinity to the mouse MD-2/TLR4 receptor complex.

Next, we tested the capability of each of these two distinct LPSs to remove already bound LPS from the receptor complex. Thus, we incubated mTLR4-HEK cells with different concentrations of either bioLPSBV or LPSEC for 1 h, and, subsequently, we added the opposite LPS for 1 h and in several concentrations. Subsequent additional incubation with phycoerythrin (PE)-coupled streptavidin (Strep-PE) allowed for flow cytometry-based visualization of mTLR4-HEK cell-bound bioLPSBV (Figure 5B). Pre-incubation with LPSEC followed by subsequent incubation with bioLPSBV resulted in a low detected PE fluorescence, fairly independent of the employed LPSEC and bioLPSBV concentrations (Figure 5C). This indicated that, once the murine MD-2/TLR4 receptor complex was bound by LPSEC, bioLPSBV was not able to remove LPSEC from the receptor-binding site. Pre-incubation with LPSEC, even at low concentrations of 1.25 mg L^{-1}, resulted in a decrease of the PE signal to about 20% of the PE signal that arose when cells were not pre-incubated with LPSEC (Figure 5C). Contrariwise, pre-incubation of mTLR4-HEK cells with bioLPSBV followed by subsequent incubation with LPSEC resulted in a strong reduction of the PE signal, which is exclusively derived from bound bioLPSBV, of about 50%, even when low concentrations of LPSEC were added (Figure 5D). Since we assumed that the detected PE fluorescence was directly proportional to the amount of bound bioLPSBV, it can be stated that bioLPSBV was able to remove about 20% of already bound LPSEC (Figure 5C), while LPSEC was able to remove about 50% of already bound bioLPSBV (Figure 5D).

We have already demonstrated that LPSBV is able to induce tolerant semi-mature BMDCs *in vitro* (Figure 3) and reduce established intestinal inflammation in T cell-transplanted *Rag1*$^{-/-}$ mice harboring a complex microbiota (Figure 4). So far, all experiments investigating smBMDCs *in vitro* were performed in the absence of other LPS structures for the first 16 h of the semi-maturation process. Physiological conditions in the colonic lumen provide the presence of different commensal LPSs in large amounts at the same time. Therefore, we stimulated BMDCs with weak agonistic LPSBV and prototype agonistic LPSEC at the same time and at different concentrations for 16 h (Figure 6A) to investigate if LPSBV-induced semi-maturation even occurs in the presence of a strong MD-2/TLR4 receptor complex agonist. Thus, we checked for the secretion of pro-inflammatory cytokines and the surface expressions of MHC class II and TLR4.

We detected a concentration-dependent effect of LPSBV stimulation on BMDCs in the absence of LPSEC (light blue lines in Figure 6B). LPSBV concentrations of up to 100 ng mL^{-1} (which equals 50 ng/10^6 BMDCs) led to a semi-mature BMDC phenotype, as

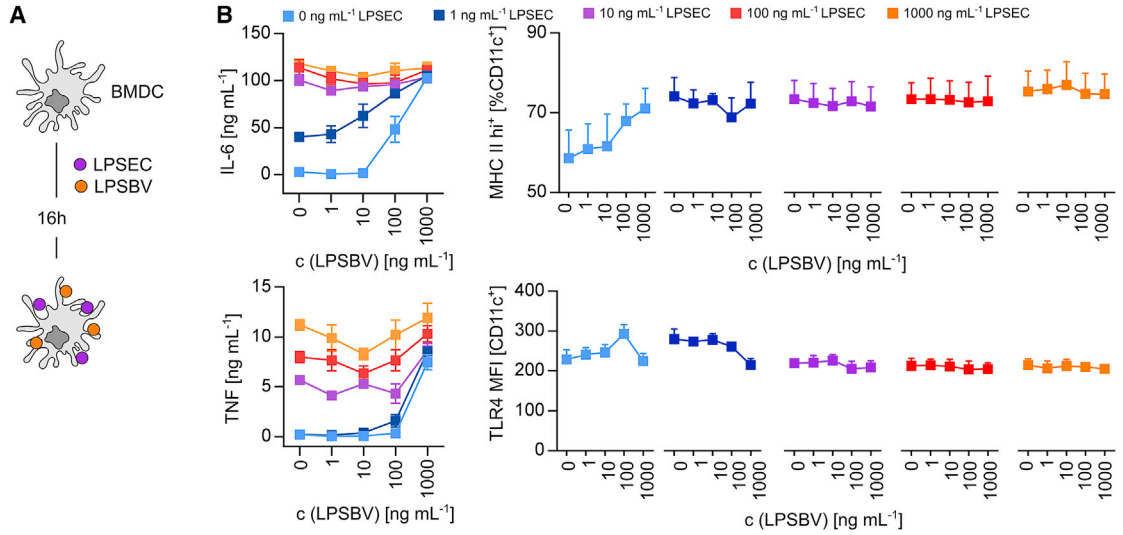

Figure 6. LPSEC-Induced BMDC Maturation Can Not Be Anticipated by the Simultaneous Presence of LPSBV *In Vitro*

(A) Experimental setting for (B): simultaneous stimulation of WT BMDCs (n = 3 mice) with LPSEC and LPSBV with varying concentrations of both LPSs. (B) Detection of cytokine secretion and surface expressions of MHC class II and TLR4 of the experimental approach depicted in (A). Cytokine secretion was detected by ELISA. Surface expressions of MHC class II and TLR4 were detected by flow cytometry. Squares with error bars represent mean ± SD.

previously demonstrated in Figure 3. Using 1,000 ng mL^{-1} or 500 ng pure LPSBV/10^6 cells resulted in a strong activation of BMDCs, as indicated by high TNF, IL-6, and MHC class II surface expressions (Figure 6B). This underlined and confirmed the observation that LPSBV is not a MD-2/TLR4 receptor complex antagonist but rather a weak agonist, with the overall concentration determining its final endotoxicity. The addition of agonistic LPSEC to LPSBV-stimulated BMDCs led to strong increases in secretion rates of pro-inflammatory cytokines (Figure 6B) as well as in the expression of MHC class II (Figure 6B) for all the used LPSEC concentrations. Therefore, the simultaneous presence of LPSBV could not anticipate LPSEC-induced maturation effects. Surprisingly, TLR4 expression on the cell surface remained relatively constant among all differently stimulated BMDCs (Figure 6B), indicating that no significant TLR4 endocytosis is detectable upon binding of these two LPS structures to the MD-2/TLR4 receptor complex, which was in opposition to what was previously reported for other intestinal commensally derived LPSs.[54]

So far, these results indicated that the simultaneous encounter of BMDCs with weak agonistic LPSBV and strong agonistic LPSEC prevented LPSBV-induced semi-maturation. However, LPSBV administration into mice harboring a complex microbiota reduced intestinal inflammation. Since LPSBV-induced semi-maturation of $CD11c^+$ cells might account for the observed inflammation-reducing effects of LPSBV *in vivo*, we were interested to know how competition between LPSBV and endogenous LPS as well as other microbial components from a complex mouse microbiota affects the phenotype of $CD11c^+$ cells. Therefore, we generated BMDCs from WT C57BL/6 mice, and we stimulated them with isolated LPSBV as described before. Simultaneously, we added autoclaved feces that were taken from *Rag1*$^{-/-}$ mice 4 weeks after T cell transplantation, which provided severe intestinal inflammation (Figure 1B). These feces, therefore, represent a DYSM composition that arises during intestinal inflammation. The DYSM harbors various endogenous LPSs competing with LPSBV for binding to the MD-2/TLR4 receptor complex on LP $CD11c^+$ cells as well as various other immunomodulating components. Additionally, the DYSM represents the microbiota composition LPSBV faced when it was administered to inflamed *Rag1*$^{-/-}$ mice and exhibited inflammation-ameliorating properties. DYSM stimulation of BMDCs resulted in slight, but not statistically significant, increases in the secretions of pro-inflammatory cytokines and T cell co-stimulatory molecules (Figure 7A). This indicated that the DYSM impacted $CD11c^+$ cell maturation, albeit not as strongly as EC with agonistic LPS (Figure S9), at least at the chosen DYSM concentration. Interestingly, simultaneous stimulation of BMDCs with DYSM and LPSBV induced significantly stronger expressions of IL-6 and TNF as well as increased surface expressions of MHC class II and CD40 than either of the stimuli administered alone.

Since simultaneous stimulation of BMDCs with DYSM and LPSBV resulted in fully mature BMDCs, we pre-incubated BMDCs with LPSBV (prime) for 24 h before adding the DYSM (challenge). As seen in Figure 7B, pre-incubation of LPSBV resulted in an induction of tolerance of IL-6 and TNF expressions, preventing the secretion of pro-inflammatory cytokines in response to DYSM challenge. However, surface expressions of MHC class II and CD40 were not altered in LPSBV-primed and DYSM-challenged BMDCs compared to unprimed and DYSM-challenged BMDCs.

These experiments demonstrate that the simultaneous stimulation of $CD11c^+$ BMDCs cells with LPSBV and components of an endogenous DYSM did not lead to semi-maturation. Therefore, we concluded that

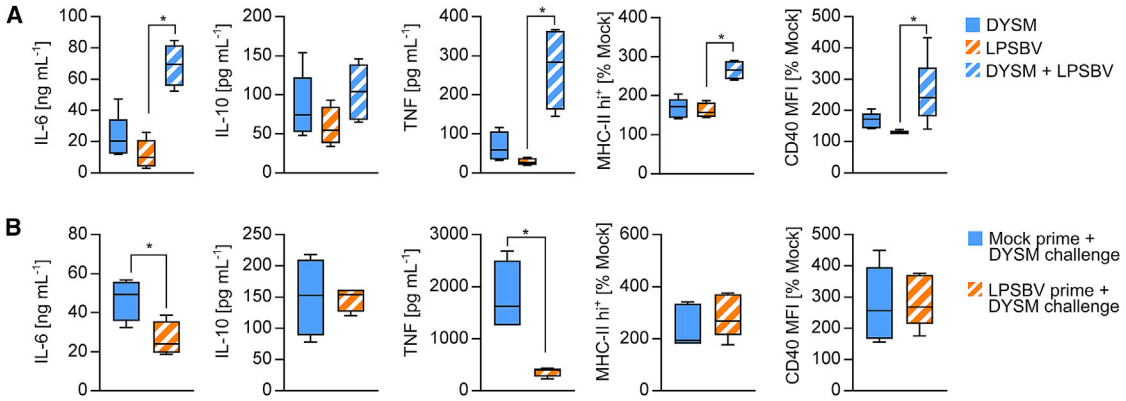

Figure 7. LPSBV-Mediated BMDC Tolerance Is Induced in the Absence of Agonistic LPS and Protects from Pro-inflammatory Response to a Dysbiotic Microbiota Composition

(A) Feces from *Rag1*$^{-/-}$ mice providing intestinal inflammation (DYSM) was autoclaved and prepared as described in the Materials and Methods. WT BMDCs (n = 4–5 mice) were stimulated with DYSM, LPSBV (100 ng mL^{-1}), or both simultaneously (DYSM + LPSBV). Cytokine secretion was detected by ELISA. Surface expressions of MHC class II and CD40 were detected by flow cytometry and normalized to the mock control of BMDCs generated from the same individual. (B) WT BMDCs were stimulated (prime) with either PBS (mock) or LPSBV for 24 h. Medium was changed and cells were stimulated afterward (challenge) with DYSM. Cytokine secretion was detected by ELISA. Surface expressions of MHC class II and CD40 were detected by flow cytometry and normalized to an unchallenged mock control of BMDCs generated from the same individual. Statistical analysis was performed using one-way ANOVA (A) or Student's t test (B). p values <0.05 were considered to be statistically significant and are indicated with an asterisk (*). Boxplots depict the mean as well as the 25th and 75th percentiles, and whiskers depict the highest and lowest values.

LPSBV-mediated induction of smBDMCs required the absence of agonistic LPS for the initial phase of semi-maturation induction.

DISCUSSION

BVMPK belongs to the gram-negative bacterial phylum *Bacteroidetes*, representing one of the two most prominent phyla in the mammalian gut.[29,30] However, the proportion of *Bacteroidetes* in the intestinal microbiota is dependent on the inflammatory status of the gut. In ulcerative colitis patients, the proportion of *Bacteroides* spp. is markedly decreased,[55] supporting the idea of *Bacteroides* spp. being important beneficial players in the intestinal microbiota. Additionally, we have already shown that the administration of BVMPK prevents disease induction in different mouse models for experimental colitis,[20–22] mainly by the induction of hyporesponsive semi-mature CD11c^{+} cells (smDCs) in the cLP. These smDCs are responsible for the prevention of pro-inflammatory immune responses.[20–22,31] In this study, we report that the administration of BVMPK drastically reduces established and ongoing pathological inflammatory processes in the intestine of a mouse model for experimental colitis using *Rag1*$^{-/-}$ mice. These immune response-regulating properties were mediated by LPSBV, as the healing effects could be obtained using purified LPSBV only. We therefore propose that LPSBV might be a novel therapeutic agent for the treatment of chronic gut inflammatory disorders, by restoring physiological intestinal immune homeostasis.

BVMPK is not the only *Bacteroides* strain that exhibits such beneficial immunomodulatory properties. BF was reported to protect against intestinal inflammation in a mouse model for experimental colitis[56] as well as against CNS demyelination and inflammation during experimental autoimmune encephalomyelitis.[48] Interestingly, these properties were mediated by one of its capsular PSAs through interaction with host TLR2.[48,56,57] So far, we have no information on the chemical structure of BVMPK capsular polysaccharides, but the close relation between BF and BVMPK and the convincing immune system-regulating properties of BF PSA prompted us to check for a contribution of TLR2 signaling to the observed immunological effects in CD11c^{+} cells in response to LPSBV stimulation. This is of particular interest since such a TLR2-mediated signaling might be due to contamination of the used LPSBV preparations with capsular polysaccharides[45–48,56,57] and lipoproteins[49–51] or due to the LPS itself.[43,44,58] Although a slight TLR2 activation was detected, LPSBV preparations crucially mediated the induction of CD11c^{+} cell semi-maturation via the MD-2/TLR4 receptor complex.

In this context, we demonstrated that the immunomodulatory properties of LPSBV are clearly distinguishable from that of strong TLR4 agonists such as, e.g., *E. coli*-derived prototype LPS, or antagonists, which block any TLR4-mediated signaling. Since LPSBV did not induce the expression of pro-inflammatory cytokines but actively induced hyporesponsiveness toward subsequent LPS stimuli in CD11c^{+} cells, thereby fairly merging the properties of TLR4 antagonists and agonists, we propose LPSBV to be a weak agonist concerning its interaction with the MD-2/TLR4 receptor complex.

To elucidate how endogenous LPSs from a complex mouse microbiota affect the phenotype of CD11c^{+} cells, we autoclaved the feces of inflamed *Rag1*$^{-/-}$ mice (DYSM). Hence, the DYSM represents the endogenous LPS composition as well as other microbial compounds LPSBV faced when it was administered to inflamed *Rag1*$^{-/-}$ mice and exhibited inflammation-ameliorating properties. Interestingly, simultaneous stimulation of BMDCs with DYSM and LPSBV induced significantly stronger expressions of IL-6 and TNF as well

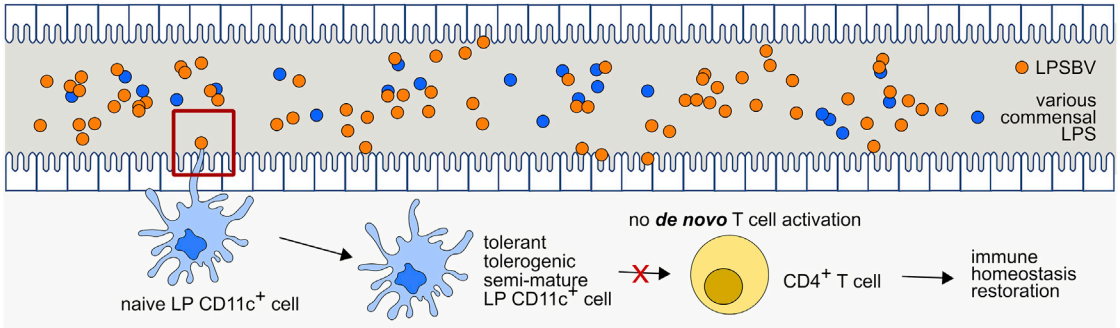

Figure 8. Proposed Mechanism of How Weakly Agonistic LPSBV Influences MD-2/TLR4 Receptor Complex Activation and Prevents the Initiation of a CD4$^+$ T Cell-Mediated Immune Response via Modulation of the Intestinal CD11c$^+$ Cells

Therapeutic administration of LPS from symbiotic *B. vulgatus* mpk ends up in large amounts in the intestine, exceeding the amount of present LPS from other intestinal commensal bacteria. Excess LPSBV primes naive CD11c$^+$ cells into a tolerant, tolerogenic, and semi-mature phenotype that fails to activate CD4$^+$ T cells. This prevention of a *de novo* activation of CD4$^+$ T cells leads to a phase-out of ongoing inflammatory processes, while *de novo* induction of an immune response is prevented. However, our data indicate that this only happens if LPSBV is the only TLR4 ligand that CD11c$^+$ cells encounter when they are still naive and immature. LPSBV needs a certain period of time to induce CD11c$^+$ cell tolerance. Simultaneous encounter with agonistic LPS does not lead to CD11c$^+$ cell tolerance, and it does not, therefore, promote abrogation of inflammatory processes.

as increased surface expressions of MHC class II and CD40 than either of the stimuli administered alone. This finding is most likely due to the fact that the induction of cytokines as well as the expression of cell surface markers follows a dose-response effect. It can be seen in Figure 6B that the stimulation of BMDCs with high concentrations of LPSBV results in the induction of TNF and IL-6 secretions. Adding LPSBV and the DYSM sample simultaneously results in the stimulation of the cells with high LPS levels, hence inducing the secretions of proinflammatory cytokines and expressions of BMDC activation surface markers. The anti-inflammatory potential of LPSBV is nicely demonstrated in Figure 7B where BMDCs were primed with either PBS (mock) or LPSBV and challenged with DYSM. In this experiment, it can be clearly seen that priming the cells with LPSBV led to reduced secretions of TNF and IL-6 upon a challenge with DYSM.

Referring to the therapeutic effects of LPSBV in efficiently reducing intestinal inflammation, we conclude that the concentration of LPSBV located in the intestinal lumen is a decisive factor and must exceed the number of endogenous agonistic LPSs in order to induce tolerant semi-mature CD11c$^+$ in the LP. Such exceeding LPSBV concentrations are thought to enhance the probability that intestinal DCs only encounter weak agonistic LPSBV by enhancing the ratio between weak agonistic to endogenous agonistic LPSs. This seems to be indispensable since we demonstrated that a simultaneous encounter with a strong agonistic LPS prevented LPSBV-induced DC semi-maturation and induced pro-inflammatory responses instead. We could further demonstrate that prototype agonistic LPSEC was able to remove already bound LPSBV from the MD-2/TLR4 receptor complex more efficiently than vice versa.

In a scenario of exceeding LPSBV concentrations in the gastrointestinal lumen, this effect is thought to be irrelevant. As demonstrated, the endotoxicity of LPSBV is dependent on its concentration, and a very high LPSBV concentration leads to complete DC maturation underlying its weak agonistic properties, clearly distinguishing it from an antagonist. Nevertheless, we demonstrated that the administration of a daily dose of about 1 mg LPSBV/mouse via the drinking water led to the observed inflammation-reducing effects in *Rag1*$^{-/-}$ mice with colitis, indicating that such a concentration is sufficient to exceed the amount of endogenous LPS in the gastrointestinal tract while simultaneously being in a semi-maturation-inducing concentration range. Once CD11c$^+$ cell semi-maturation is induced, this phenotype cannot be overcome, and it is, therefore, thought to result in the prevention of a *de novo* T cell activation in the intestine. Therefore, after a phase-out of ongoing inflammatory processes, newly induced semi-mature DCs through LPSBV administration would prevent a continuous T cell activation (Figure 8) and, therefore, promote healing of damaged colonic tissue.

In general, LPS is a potent MD-2/TLR4 receptor complex agonist leading to strong intracellular signaling in target cells, resulting in the transcription of genes associated with pro-inflammatory immune responses.[13] LPS-induced strength of this intracellular signaling is widely considered to be mostly mediated by its lipid A portion.[59,60]

Lipid A structures of various *Bacteroides* spp. were already reported to harbor 4–5 acyl chains and only 0–1 phosphate group.[8] Since we revealed strong genetic similarities between the lipid A synthesis core of BVMPK and other *Bacteroides* spp., we suggest LPSBV also to be hypo-acylated and hypo-phosphorylated compared to LPSEC. Hexa-acylated and *bis*-phosphorylated *E. coli* lipid A is considered to be the most potent activator of the MD-2/TLR4 receptor complex-mediated signaling, since it was demonstrated that five of the six acyl chains are buried inside the MD-2-binding cavity while the sixth acyl chain points out to the MD-2 surface-mediating hydrophobic interactions with the TLR4 ectodomain, which are necessary for TLR4 activation.[12,34] This might partly explain the lower endotoxicity of hypo-acylated lipid A structures lacking this sixth acyl chain and

the weak agonistic activity of hypo-acylated LPSBV. Furthermore, both 1- and 4'- phosphates on the lipid A diglucosamine backbone were demonstrated to be important moieties for MD-2/TLR4 receptor complex activation.[13] Since *Bacteroidales* possessed only one phosphate at position 1 of the reducing glucosamine,[8] this may also contribute to its weakly agonistic effects, as a missing 4'-phosphate was demonstrated to result in a 100-fold reduction in endotoxic activity.[61]

We suppose the weak agonistic features of LPSBV to be responsible for the observed healing effects in mice with intestinal inflammation. In this context, weak agonistic LPS is thought to induce a weaker, but still detectable, intracellular signaling and NF-κB activation, providing a basic anti-inflammatory intracellular transcription program without exceeding a pro-inflammatory threshold. Furthermore, LPSBV leads to the active induction of hyporesponsive $CD11c^+$ cells. These properties clearly distinguish LPSBV from strong agonistic LPSEC, which induces endotoxin tolerance but also strong pro-inflammatory signaling. However, weak agonistic LPS is also different from antagonistic LPS, which does not promote pro-inflammatory reactions but also does not promote tolerance induction in TLR4-expressing cells. The property of LPSBV of being an effective ligand for the MD-2/TLR4 receptor complex and, at the same time, a weak agonist must, of course, be attributed to its chemical structure. We think that this is a chemical paradigm of the commensal intestinal microbiota LPS, contributing to the adaption of microbes to the host. In line with this, other groups reported on the contribution of *Bacteroides* LPS to the preservation of intestinal homeostasis.[8] However, our study represents the first successful attempt to actively restore intestinal immune homeostasis in mice providing severe intestinal inflammation by using commensally derived LPS.

However, the immunogenic effects of weak agonistic LPS seem to be situation dependent. In another study, Vatanen et al.[33] revealed a higher incidence of type 1 diabetes (T1D) in children who were less exposed to strong agonistic LPS in early childhood, accompanied by higher proportions of microbes harboring hypo-acylated and hypo-phosphorylated LPS. In line with this, continuous intraperitoneal administration of *E. coli* LPS starting shortly after birth delayed the onset of T1D in non-obese diabetic (NOD)/Shilt mice while the administration of hypo-acylated and hypo-phosphorylated BD LPS failed to do so.[33] This study supported the hygiene hypothesis that assumes that early exposure to highly immunogenic microorganisms in early childhood benefits immune system development and protects the host from allergic and autoimmune diseases. At first sight, these observations seem to be contradictory to our results. Though, in our study, we aimed to actively re-establish immune homeostasis from severe intestinal inflammation in adult animals. This approach is different from the aim to protect from spontaneous disease onset through microbiota modulation in infants. Additionally, other groups consider hypo-phosphorylated and hypo-acylated *Bacteroides* LPS to be antagonistic. However, we have clearly demonstrated that these LPS structures rather act as weak agonists.

Our results and those of other groups raise the question of the potential use of weak agonistic LPS as a suitable therapeutical tool to restore homeostatic conditions not only in experimental mouse models but also in IBD patients. Therapy of IBD patients is, to date, restricted to a general suppression of the patient's immune response, often associated with undesirable side effects. LPS (derivative)-based treatment might avoid this problem by acting only locally at the site of inflammation, the intestine.

Although our results strongly indicate a direct LPS-mediated modulation of $CD11c^+$ cells in the intestinal LP to be the key driver for the observed healing effects, we cannot completely rule out that the re-establishment of intestinal homeostasis only represents a secondary effect in response to a potential LPSBV-induced microbiota shift from dysbiotic to homeostatic.

Nevertheless, we aim to promote purified LPSBV as an alternative for the treatment of intestinal inflammatory disorders or IBD, providing evidence that this compound demonstrated its beneficial effects as not being an antagonist but rather a weak agonist. Concluding, we contribute this study to IBD therapy-related research, offering a completely new approach that avoids the disadvantages of current state-of-the-art IBD therapies.

MATERIALS AND METHODS

Mice

C57BL/6 mice were purchased from Charles River Laboratories, and C57BL/6J-*Rag1*^{tm1Mom} (*Rag1*$^{-/-}$) mice were obtained from our own breeding. All animals were kept and bred under specific pathogen-free (SPF) conditions in individually ventilated cages (IVCs), receiving standard chow and regular drinking water. For the isolation of bone marrow from C57BL/6 mice, only female mice aged 6–12 weeks were used. *Rag1*$^{-/-}$ mice were used as a mouse model for T cell transplantation-dependent experimental chronic colitis. Animal experiments were reviewed and approved by the responsible institutional review committee and the local authorities (Regierungspräsidium Tübingen, Permit H6/10, Anzeigen 01.12.11, 09.01.15, 14.06.17).

T Cell-Mediated Induction of Chronic Colitis in *Rag1*$^{-/-}$ Mice

C57BL/6J-*Rag1*^{tm1Mom} (*Rag1*$^{-/-}$) mice were transplanted with 5×10^5 splenic $CD4^+CD62L^+CD45RB^{hi}$C WT T cells at 8–10 weeks of age. *Rag1*$^{-/-}$ mice harbored a so-called DYSM, which efficiently triggers the induction of pathological intestinal inflammation upon transplantation of naive T cells, as reported previously.[7,22] This microbiota was absent of Norovirus, Rotavirus, and *Helicobacter hepaticus*. Furthermore, detailed next-generation sequencing-based analysis of DYSM composition revealed a significantly increased relative abundance of the bacterial phyla *Proteobacteria*, *Verrucomicrobia*, and *Firmicutes*, while the relative abundance of *Bacteroidetes* was drastically reduced compared to a symbiotic microbiota composition, as published previously by our group.[7] During the experiments, *Rag1*$^{-/-}$ mice were kept under SPF conditions in IVCs and analyzed 8 weeks after T cell transplantation, as indicated in the Results.

Radiopharmaceuticals

[^{18}F]fluoride was produced by using ^{18}O (p,n) ^{18}F nuclear reaction on the PETtrace cyclotron (General Electric Medical Systems, GEMS, Uppsala, Sweden). [^{18}F]FDG synthesis was performed as described elsewhere.[62] After the synthesis, specific activity was calculated and revealed to be >50 GBq/mmol with a radiochemical purity of >99%.

In Vivo PET Imaging

High-resolution PET imaging was performed using two identical small animal Inveon microPET scanner (Siemens Medical Solutions, Knoxville, USA) with a spatial resolution of 1.4 mm in the reconstructed images (field of view [FOV]: transaxial, 10 cm; axial, 12.7 cm).[63] By applying iterative ordered subset expectation maximization (OSEM) 2D algorithm for reconstruction, list mode data were processed. Mice were anesthetized with 1.5% isoflurane (Abbott, Wiesbaden, Germany) vaporized with O_2 (1.5 L/min) and injected intravenously (i.v.) into the tail vein with 8.3 ± 1.3 MBq [^{18}F]FDG. After tracer injection, animals were kept anesthetized for 60 min, in an anesthesia box, placed on a heating pad to maintain body temperature of animals during tracer uptake time. Shortly before the end of the uptake time, mice were placed in the FOV of the PET scanner on a warmed (37°C) scanner bed. Static (10-min) PET scans were performed on weeks 0, 4, 6, and 8 after T cell application. Data were corrected for decay, normalized to the injected activity, and analyzed using Pmod Software (PMOD Technologies, Zurich, Switzerland) by drawing regions of interest over the intestine.

Bacteria

The bacteria used for stimulation of the mouse BMDCs were EC and BVMPK, which were described in detail previously.[20–22,31,64] Additionally, we used BD CL02T12C06, BTIO VPI-5482, BV8482 ATCC 8482, and BF ATCC 25285, DSM 2151. The EC strain was grown in Luria-Bertani (LB) medium under aerobic conditions at 37°C. All *Bacteroides* strains were grown in brain-heart-infusion (BHI) medium and anaerobic conditions at 37°C.

Comparison of *Bacteroides* spp. Lipid A Synthesis Genes

Lipid A synthesis genes were identified in BVMPK (GenBank: NZ_CP013020.1) using the *B. vulgatus* ATCC8482 type strain genome sequence (GenBank: NC_009614.1). The amino acid sequences of all lipid A synthesis enzymes of BVMPK were subsequently compared to BD CL02T12C06 (GenBank: NZ_AGXJ00000000.1), BTIO VPI-5482 (GenBank: NC_004663.1), BF NCTC 9343 (GenBank: NC_003228.3), and *E. coli* K12 MG1655 (GenBank: NC_000913.3), using the standard protein BLAST (blastp suite).

Isolation of LPSBV and LPSEC

The lyophilized bacterial pellet was washed several times with distilled water, ethanol, and acetone, followed by several ultracentrifugation steps (45,000 rpm at 4°C) in order to remove cell, growth broth, and capsular contaminants.

Cells were extracted by hot phenol-water extraction.[65] Water and phenol phases were both exhaustively dialyzed and lyophilized. After inspection by SDS-PAGE, an enzymatic treatment to remove proteins and nucleic acids was executed, followed by a dialysis step. The SDS-PAGE executed on both purified water and phenol phases highlighted the presence of LPS only in the water phase from which it was further purified.

Biotinylation of LPSBV

10 mg LPSBV was biotinylated with EZ-Link Micro Sulfo-NHS-LC-Biotinylation Kit (Thermo Scientific), according to the manufacturer's protocol, using PBS as a solvent. To remove PBS, an exhaustive dialysis against distilled water was performed. The biotinylated LPS_{BV} ($bioLPS_{BV}$) was then collected and lyophilized. For *in vitro* experiments, lyophilized $bioLPS_{BV}$ was dissolved in distilled water in concentrations not higher than 1 mg mL^{-1}.

Cultivation of BMDCs

Bone marrow cells were isolated from C57BL/6 WT, TLR2-deficient, TLR4-deficient, and TLR2 × TLR4 double-deficient mice and cultivated as described previously.[66] At day 7 after isolation, the resulting CD11c-positive dendritic cells were used for stimulation experiments.

Stimulation of BMDCs

2×10^6 BMDCs were stimulated with PBS, BVMPK, or EC at an MOI of 1 or the respective isolated LPS at concentrations as indicated in the Results. Cells were stimulated for a maximum of 24 h. If viable bacteria were used for stimulation, gentamycin was added at a final concentration of 1 μg mL^{-1} to avoid bacterial overgrowth under aerobic conditions. If a second challenge was used, cells were stimulated with bacteria or LPS preparations for 24 h. Cell culture medium was changed before challenging the cells with a second stimulus for a maximum of additional 16 h. PBS was used as a mock stimulation control. For stimulation with a DYSM composition, feces were collected from living SPF *Rag1*$^{-/-}$ animals exhibiting severe intestinal inflammation, 4 weeks after T cell transplantation. Feces were autoclaved for 15 min at 121°C and weighed, and sterile PBS was added to obtain a final concentration of 50 mg mL^{-1}. Homogemnized feces were then filtered through a 100-μm sieve. The filtered suspension was diluted by a factor of 2.5, and 5 μL was added to 1 mL cell culture medium containing 10^6 BMDCs. The competitive TLR4 antagonist TAK242 was added at a final concentration of 10 μM at 1 h prior to stimulation with LPS, $Pam2CSK_4$, flagellin from *S.* Typhimurium (FLA-ST), or viable bacteria.

Stimulation of HEK Cells

2×10^5 HEK cells expressing murine CD14, MD-2, and TLR4 (mTLR4-HEK) in 1 mL medium were stimulated with 1–1,000 ng mL^{-1} isolated LPS or bacteria (MOI 1) for the time points indicated in the Results.

Detection of Bound Biotinylated LPSBV

After incubation with biotinylated LPSBV, mTLR4-HEK cells were scraped off, washed once in PBS + 1% fetal calf serum (FCS), and

incubated with Strep-PE for 30 min, followed by another washing step. Cell-attached Strep-PE was detected by flow cytometry. All experiments to be compared were carried out in one experimental setting to guarantee for comparability of the detected MFI (median fluorescence intensity) values of the PE fluorescence.

Cytokine Analysis by ELISA

For the analysis of secreted cytokines (IL-6, IL-10, and TNF), ELISA-based detection kits were purchased from BD Biosciences and used according to the manufacturer's instructions.

Flow Cytometry Analysis

Multi-color flow cytometrical (FCM) analyses were performed on a FACS Calibur or FACS LSRII (BD Biosciences). All fluorochrome-coupled antibodies were purchased from BD Biosciences if not stated otherwise. Data were analyzed using the FlowJo software (Tree Star, USA).

ALDH Activity Assay

Intracellular ALDH activity in BMDCs was assayed using the Aldefluor kit (STEMCELL Technologies), according to the manufacturer's instructions. Samples treated with the specific ALDH inhibitor diethylaminobenzaldehyde (DEAB) served for the determination of baseline fluorescence and defining ALDH-positive cells (Figure S5).

Purification of RNA and Quantitative Real-Time PCR

Purification of RNA from colonic scrapings was performed using QIAGEN's RNeasy Mini Kit, according to the manufacturer's instructions. Additional DNA digestion was conducted by using 4 U rDNase I and 40 U rRNasin for an RNA solution of 0.1 μg μL^{-1}. After 30 min of incubation at room temperature (RT), DNase was inactivated using Ambion DNase inactivation reagent, which was later removed by centrifugation for 1 min at 10,000 × *g*. SybrGreen-based qRT-PCR was performed on a Roche LightCycler480 using QIAGEN SybrGreen RT-PCR Kit. Primer annealing occurred at 60°C. 10–100 ng DNA-digested RNA was used for qRT-PCR. Relative mRNA expression in BMDCs stimulated with bacteria to unstimulated BMDCs was determined, with β-actin as the housekeeping gene, using the ΔΔCp method that included the specific amplification efficiency of every used primer pair and each PCR run.

Primer Sequences

Primers used for qRT-PCR were as follows: Aldh1a2 forward, 5′-AAGACACGAGCCCATTGGAG-3′; reverse, 5′-GGAAAGCCAGCCTCCTTGAT-3′; and β-actin forward, 5′-CCCTGTGCTGCTCACCGA-3′; reverse, 5′-ACAGTGTGGGTGACCCCGTC-3′.

Isolation of LP DCs and T Cells and the Adoptive Transfer of T Cells

Isolation of LP cells was performed as reported previously.[67] For adoptive transfer, splenic $CD4^+$ T cells from C57BL/6 mice were purified using a magnetic-activated cell sorting (MACS)-based negative selection kit (Miltenyi), according to the manufacturer's instructions. The isolated cells were stained for CD3ε, CD4, CD62, and CD45RB for reanalysis; purity was generally >90% with >80% being $CD3\varepsilon^+CD4^+CD62L^+CD45RB^{hi}$. 5×10^5 $CD4^+$ T cells were injected intraperitoneally (i.p.) into *Rag1*$^{-/-}$ mice, as described previously.[68]

Histology

Colonic tissues were fixed in neutral buffered 4% formalin. Formalin-fixed tissues were embedded in paraffin and cut into 2-μm sections. They were stained with H&E (Merck) for histological scoring. Scoring was conducted in a blinded fashion on a validated scale of 0–3, with 0 representing no inflammation and 3 representing severe inflammation characterized by infiltration with inflammatory cells, crypt hyperplasia, loss of goblet cells, and distortion of architecture.[69]

Antibodies

The following antibodies were used for flow cytometry analysis of intracellular and surface proteins: anti-mouse CD11c-allophycocyanin (APC) (clone H3; Becton Dickinson), anti-mouse MHC class II-fluorescein isothiocyanate (FITC) (clone 2G9, Becton Dickinson), anti-mouse MHC class II-BV510 (clone 2G9, Becton Dickinson), anti-mouse CD40-FITC (clone 3/23, Becton Dickinson), anti-mouse CD40-BV421 (clone 3/23, Becton Dickinson), anti-mouse CD80-FITC (clone B7-1 (16-10A1), Becton Dickinson), anti-mouse CD86-FITC (clone GL1, Becton Dickinson), anti-mouse p65-PE (pS534) (clone 96H1, Becton Dickinson), anti-mouse Ly6G/Ly6C-FITC (clone GR-1/RB-68C5, Becton Dickinson), anti-mouse CD45R-FITC (clone RA3-6B2, Becton Dickinson), anti-mouse CD64-FITC (clone X54-5/7.1, Becton Dickinson), anti-mouse CD45-BV421 (clone 30-F11, Becton Dickinson), anti-mouse CD11b-BV605 (clone M1/70, Becton Dickinson), anti-mouse CD103-PerCP-Cy5.5 (clone M290, Becton Dickinson), and anti-mouse TLR4-biotin (clone SA15-21, BioLegend).

Statistics

For comparisons of two groups, a parametric Student's t test was used for normally distributed values. For multiple comparison of more than two groups, one-way ANOVA was used for normally distributed values and non-parametric Kruskal-Wallis test was used elsewhere. p values are indicated in the figures; p values <0.05 were considered to be significant.

SUPPLEMENTAL INFORMATION

Supplemental Information can be found online at https://doi.org/10.1016/j.ymthe.2019.07.007.

AUTHOR CONTRIBUTIONS

Conceptualization, A.S., J.-S.F., L.M., and A.M.; Methodology, A.S., F.D.L., and A.M.; Formal Analysis, A.S. and L.M.; Investigation and Data Curation, A.S., L.M., F.D.L., T.K., T.M., J.K.M., A.S., A.L., R.P., K.G., K.F., A.S., and H.H.Ö.; Resources, F.D.L., K.F., B.J.P., and A.M.; Writing – Original Draft, A.S., I.B.A., A.M., and J.-S.F.; Writing – Review & Editing, A.S., L.M., I.B.A., A.M., and J.-S.F.; Visualization, A.S. and L.M.; Supervision, I.B.A. and J.-S.F.; Project Administration, A.S., J.-S.F., and L.M.; Funding Acquisition, J.-S.F.

CONFLICTS OF INTEREST

The authors declare no competing interests.

ACKNOWLEDGMENTS

This work was funded by the Deutsche Forschungsgemeinschaft (DFG, German Research Foundation) under Germany's Excellence Strategy – EXC-2124 and Collaborative Research Centres 685 (CRC685), the DFG research training group 1708, the Bundesministerium für Bildung und Forschung (BMBF), and the German Center for Infection Research (DZIF).

REFERENCES

1. Herfarth, H., and Rogler, G. (2005). Inflammatory bowel disease. Endoscopy *37*, 42–47.
2. Jostins, L., Ripke, S., Weersma, R.K., Duerr, R.H., McGovern, D.P., Hui, K.Y., Lee, J.C., Schumm, L.P., Sharma, Y., Anderson, C.A., et al.; International IBD Genetics Consortium (IIBDGC) (2012). Host-microbe interactions have shaped the genetic architecture of inflammatory bowel disease. Nature *491*, 119–124.
3. Abegunde, A.T., Muhammad, B.H., Bhatti, O., and Ali, T. (2016). Environmental risk factors for inflammatory bowel diseases: Evidence based literature review. World J. Gastroenterol. *22*, 6296–6317.
4. Duboc, H., Rajca, S., Rainteau, D., Benarous, D., Maubert, M.A., Quervain, E., Thomas, G., Barbu, V., Humbert, L., Despras, G., et al. (2013). Connecting dysbiosis, bile-acid dysmetabolism and gut inflammation in inflammatory bowel diseases. Gut *62*, 531–539.
5. Peyrin-Biroulet, L., Van Assche, G., Gómez-Ulloa, D., García-Álvarez, L., Lara, N., Black, C.M., and Kachroo, S. (2017). Systematic review of tumor necrosis factor antagonists in extraintestinal manifestations in inflammatory bowel disease. Clin. Gastroenterol. Hepatol. *15*, 25–36.e27.
6. Bragazzi, N.L., Watad, A., Brigo, F., Adawi, M., Amital, H., and Shoenfeld, Y. (2017). Public health awareness of autoimmune diseases after the death of a celebrity. Clin. Rheumatol. *36*, 1911–1917.
7. Gronbach, K., Flade, I., Holst, O., Lindner, B., Ruscheweyh, H.J., Wittmann, A., Menz, S., Schwiertz, A., Adam, P., Stecher, B., et al. (2014). Endotoxicity of lipopolysaccharide as a determinant of T-cell-mediated colitis induction in mice. Gastroenterology *146*, 765–775.
8. d'Hennezel, E., Abubucker, S., Murphy, L.O., and Cullen, T.W. (2017). Total Lipopolysaccharide from the Human Gut Microbiome Silences Toll-Like Receptor Signaling. mSystems *2*, e00046-17.
9. Alexander, C., and Rietschel, E.T. (2001). Bacterial lipopolysaccharides and innate immunity. J. Endotoxin Res. *7*, 167–202.
10. Steimle, A., Autenrieth, I.B., and Frick, J.S. (2016). Structure and function: Lipid A modifications in commensals and pathogens. Int. J. Med. Microbiol. *306*, 290–301.
11. Silipo, A., Leone, M.R., Lanzetta, R., Parrilli, M., Lackner, G., Busch, B., Hertweck, C., and Molinaro, A. (2012). Structural characterization of two lipopolysaccharide O-antigens produced by the endofungal bacterium Burkholderia sp. HKI-402 (B4). Carbohydr. Res. *347*, 95–98.
12. Molinaro, A., Holst, O., Di Lorenzo, F., Callaghan, M., Nurisso, A., D'Errico, G., Zamyatina, A., Peri, F., Berisio, R., Jerala, R., et al. (2015). Chemistry of lipid A: at the heart of innate immunity. Chemistry *21*, 500–519.
13. Park, B.S., Song, D.H., Kim, H.M., Choi, B.S., Lee, H., and Lee, J.O. (2009). The structural basis of lipopolysaccharide recognition by the TLR4-MD-2 complex. Nature *458*, 1191–1195.
14. Foster, S.L., Hargreaves, D.C., and Medzhitov, R. (2007). Gene-specific control of inflammation by TLR-induced chromatin modifications. Nature *447*, 972–978.
15. Cavaillon, J.M., and Adib-Conquy, M. (2006). Bench-to-bedside review: endotoxin tolerance as a model of leukocyte reprogramming in sepsis. Crit. Care *10*, 233.
16. Biswas, S.K., and Lopez-Collazo, E. (2009). Endotoxin tolerance: new mechanisms, molecules and clinical significance. Trends Immunol. *30*, 475–487.
17. Wolk, K., Kunz, S., Crompton, N.E., Volk, H.D., and Sabat, R. (2003). Multiple mechanisms of reduced major histocompatibility complex class II expression in endotoxin tolerance. J. Biol. Chem. *278*, 18030–18036.
18. Wolk, K., Döcke, W.D., von Baehr, V., Volk, H.D., and Sabat, R. (2000). Impaired antigen presentation by human monocytes during endotoxin tolerance. Blood *96*, 218–223.
19. Steimle, A., and Frick, J.S. (2016). Molecular Mechanisms of Induction of Tolerant and Tolerogenic Intestinal Dendritic Cells in Mice. J. Immunol. Res. *2016*, 1958650.
20. Waidmann, M., Bechtold, O., Frick, J.S., Lehr, H.A., Schubert, S., Dobrindt, U., Loeffler, J., Bohn, E., and Autenrieth, I.B. (2003). *Bacteroides vulgatus* protects against *Escherichia coli*-induced colitis in gnotobiotic interleukin-2-deficient mice. Gastroenterology *125*, 162–177.
21. Müller, M., Fink, K., Geisel, J., Kahl, F., Jilge, B., Reimann, J., Mach, N., Autenrieth, I.B., and Frick, J.S. (2008). Intestinal colonization of IL-2 deficient mice with non-colitogenic B. vulgatus prevents DC maturation and T-cell polarization. PLoS ONE *3*, e2376.
22. Steimle, A., Gronbach, K., Beifuss, B., Schäfer, A., Harmening, R., Bender, A., Maerz, J.K., Lange, A., Michaelis, L., Maurer, A., et al. (2016). Symbiotic gut commensal bacteria act as host cathepsin S activity regulators. J. Autoimmun. *75*, 82–95.
23. Coyne, M.J., Zitomersky, N.L., McGuire, A.M., Earl, A.M., and Comstock, L.E. (2014). Evidence of extensive DNA transfer between bacteroidales species within the human gut. MBio *5*, e01305–e01314.
24. Mazmanian, S.K., Round, J.L., and Kasper, D.L. (2008). A microbial symbiosis factor prevents intestinal inflammatory disease. Nature *453*, 620–625.
25. Morrissey, P.J., Charrier, K., Braddy, S., Liggitt, D., and Watson, J.D. (1993). CD4+ T cells that express high levels of CD45RB induce wasting disease when transferred into congenic severe combined immunodeficient mice. Disease development is prevented by cotransfer of purified CD4+ T cells. J. Exp. Med. *178*, 237–244.
26. Rigoni, R., Grassi, F., Villa, A., and Cassani, B. (2016). RAGs and BUGS: An alliance for autoimmunity. Gut Microbes *7*, 503–511.
27. Kiesler, P., Fuss, I.J., and Strober, W. (2015). Experimental Models of Inflammatory Bowel Diseases. Cell. Mol. Gastroenterol. Hepatol. *1*, 154–170.
28. Pellegrino, D., Bonab, A.A., Dragotakes, S.C., Pitman, J.T., Mariani, G., and Carter, E.A. (2005). Inflammation and infection: imaging properties of 18F-FDG-labeled white blood cells versus 18F-FDG. J. Nucl. Med. *46*, 1522–1530.
29. Kamada, N., Chen, G.Y., Inohara, N., and Núñez, G. (2013). Control of pathogens and pathobionts by the gut microbiota. Nat. Immunol. *14*, 685–690.
30. Chassaing, B., and Darfeuille-Michaud, A. (2011). The commensal microbiota and enteropathogens in the pathogenesis of inflammatory bowel diseases. Gastroenterology *140*, 1720–1728.
31. Frick, J.S., Zahir, N., Müller, M., Kahl, F., Bechtold, O., Lutz, M.B., Kirschning, C.J., Reimann, J., Jilge, B., Bohn, E., and Autenrieth, I.B. (2006). Colitogenic and non-colitogenic commensal bacteria differentially trigger DC maturation and Th cell polarization: an important role for IL-6. Eur. J. Immunol. *36*, 1537–1547.
32. Jacobson, A.N., Choudhury, B.P., and Fischbach, M.A. (2018). The Biosynthesis of Lipooligosaccharide from *Bacteroides thetaiotaomicron*. MBio *9*, e02289-17.
33. Vatanen, T., Kostic, A.D., d'Hennezel, E., Siljander, H., Franzosa, E.A., Yassour, M., Kolde, R., Vlamakis, H., Arthur, T.D., Hämäläinen, A.M., et al.; DIABIMMUNE Study Group (2016). Variation in Microbiome LPS Immunogenicity Contributes to Autoimmunity in Humans. Cell *165*, 1551.
34. Weintraub, A., Zähringer, U., Wollenweber, H.W., Seydel, U., and Rietschel, E.T. (1989). Structural characterization of the lipid A component of Bacteroides fragilis strain NCTC 9343 lipopolysaccharide. Eur. J. Biochem. *183*, 425–431.
35. Matsunaga, N., Tsuchimori, N., Matsumoto, T., and Ii, M. (2011). TAK-242 (resatorvid), a small-molecule inhibitor of Toll-like receptor (TLR) 4 signaling, binds selectively to TLR4 and interferes with interactions between TLR4 and its adaptor molecules. Mol. Pharmacol. *79*, 34–41.
36. Ii, M., Matsunaga, N., Hazeki, K., Nakamura, K., Takashima, K., Seya, T., Hazeki, O., Kitazaki, T., and Iizawa, Y. (2006). A novel cyclohexene derivative, ethyl (6R)-6-[N-(2-Chloro-4-fluorophenyl)sulfamoyl]cyclohex-1-ene-1-carboxylate (TAK-242), selectively inhibits toll-like receptor 4-mediated cytokine production through suppression of intracellular signaling. Mol. Pharmacol. *69*, 1288–1295.

37. Roebuck, K.A. (1999). Regulation of interleukin-8 gene expression. J. Interferon Cytokine Res. *19*, 429–438.

38. Ahmed, A.U., Sarvestani, S.T., Gantier, M.P., Williams, B.R., and Hannigan, G.E. (2014). Integrin-linked kinase modulates lipopolysaccharide- and Helicobacter pylori-induced nuclear factor κB-activated tumor necrosis factor-α production via regulation of p65 serine 536 phosphorylation. J. Biol. Chem. *289*, 27776–27793.

39. Chen, L.F., Williams, S.A., Mu, Y., Nakano, H., Duerr, J.M., Buckbinder, L., and Greene, W.C. (2005). NF-kappaB RelA phosphorylation regulates RelA acetylation. Mol. Cell. Biol. *25*, 7966–7975.

40. Bazewicz, C.G., Dinavahi, S.S., Schell, T.D., and Robertson, G.P. (2019). Aldehyde dehydrogenase in regulatory T-cell development, immunity and cancer. Immunology *156*, 47–55.

41. Agace, W.W., and Persson, E.K. (2012). How vitamin A metabolizing dendritic cells are generated in the gut mucosa. Trends Immunol. *33*, 42–48.

42. Hall, J.A., Grainger, J.R., Spencer, S.P., and Belkaid, Y. (2011). The role of retinoic acid in tolerance and immunity. Immunity *35*, 13–22.

43. Chavarría-Velázquez, C.O., Torres-Martínez, A.C., Montaño, L.F., and Rendón-Huerta, E.P. (2018). TLR2 activation induced by H. pylori LPS promotes the differential expression of claudin-4, -6, -7 and -9 via either STAT3 and ERK1/2 in AGS cells. Immunobiology *223*, 38–48.

44. Nativel, B., Couret, D., Giraud, P., Meilhac, O., d'Hellencourt, C.L., Viranaïcken, W., and Da Silva, C.R. (2017). Porphyromonas gingivalis lipopolysaccharides act exclusively through TLR4 with a resilience between mouse and human. Sci. Rep. *7*, 15789.

45. Hashimoto, M., Waki, J., Nakayama-Imaohji, H., Ozono, M., Hashiguchi, S., and Kuwahara, T. (2017). TLR2-stimulating contaminants in glycoconjugate fractions prepared from Bacteroides fragilis. Innate Immun. *23*, 449–458.

46. Zughaier, S.M. (2011). Neisseria meningitidis capsular polysaccharides induce inflammatory responses via TLR2 and TLR4-MD-2. J. Leukoc. Biol. *89*, 469–480.

47. Graveline, R., Segura, M., Radzioch, D., and Gottschalk, M. (2007). TLR2-dependent recognition of Streptococcus suis is modulated by the presence of capsular polysaccharide which modifies macrophage responsiveness. Int. Immunol. *19*, 375–389.

48. Wang, Y., Telesford, K.M., Ochoa-Repáraz, J., Haque-Begum, S., Christy, M., Kasper, E.J., Wang, L., Wu, Y., Robson, S.C., Kasper, D.L., and Kasper, L.H. (2014). An intestinal commensal symbiosis factor controls neuroinflammation via TLR2-mediated CD39 signalling. Nat. Commun. *5*, 4432.

49. Hirschfeld, M., Kirschning, C.J., Schwandner, R., Wesche, H., Weis, J.H., Wooten, R.M., and Weis, J.J. (1999). Cutting edge: inflammatory signaling by Borrelia burgdorferi lipoproteins is mediated by toll-like receptor 2. J. Immunol. *163*, 2382–2386.

50. Lee, H.K., Lee, J., and Tobias, P.S. (2002). Two lipoproteins extracted from Escherichia coli K-12 LCD25 lipopolysaccharide are the major components responsible for Toll-like receptor 2-mediated signaling. J. Immunol. *168*, 4012–4017.

51. Fisette, P.L., Ram, S., Andersen, J.M., Guo, W., and Ingalls, R.R. (2003). The Lip lipoprotein from Neisseria gonorrhoeae stimulates cytokine release and NF-kappaB activation in epithelial cells in a Toll-like receptor 2-dependent manner. J. Biol. Chem. *278*, 46252–46260.

52. Bachmanov, A.A., Reed, D.R., Beauchamp, G.K., and Tordoff, M.G. (2002). Food intake, water intake, and drinking spout side preference of 28 mouse strains. Behav. Genet. *32*, 435–443.

53. Iwasaki, A., and Medzhitov, R. (2015). Control of adaptive immunity by the innate immune system. Nat. Immunol. *16*, 343–353.

54. Tan, Y., Zanoni, I., Cullen, T.W., Goodman, A.L., and Kagan, J.C. (2015). Mechanisms of Toll-like Receptor 4 Endocytosis Reveal a Common Immune-Evasion Strategy Used by Pathogenic and Commensal Bacteria. Immunity *43*, 909–922.

55. Kumari, R., Ahuja, V., and Paul, J. (2013). Fluctuations in butyrate-producing bacteria in ulcerative colitis patients of North India. World J. Gastroenterol. *19*, 3404–3414.

56. Dasgupta, S., Erturk-Hasdemir, D., Ochoa-Reparaz, J., Reinecker, H.C., and Kasper, D.L. (2014). Plasmacytoid dendritic cells mediate anti-inflammatory responses to a gut commensal molecule via both innate and adaptive mechanisms. Cell Host Microbe *15*, 413–423.

57. Ochoa-Repáraz, J., Mielcarz, D.W., Wang, Y., Begum-Haque, S., Dasgupta, S., Kasper, D.L., and Kasper, L.H. (2010). A polysaccharide from the human commensal Bacteroides fragilis protects against CNS demyelinating disease. Mucosal Immunol. *3*, 487–495.

58. Sun, K.Y., Xu, D.H., Xie, C., Plummer, S., Tang, J., Yang, X.F., and Ji, X.H. (2017). Lactobacillus paracasei modulates LPS-induced inflammatory cytokine release by monocyte-macrophages via the up-regulation of negative regulators of NF-kappaB signaling in a TLR2-dependent manner. Cytokine *92*, 1–11.

59. Brandenburg, K., Mayer, H., Koch, M.H., Weckesser, J., Rietschel, E.T., and Seydel, U. (1993). Influence of the supramolecular structure of free lipid A on its biological activity. Eur. J. Biochem. *218*, 555–563.

60. Seydel, U., Oikawa, M., Fukase, K., Kusumoto, S., and Brandenburg, K. (2000). Intrinsic conformation of lipid A is responsible for agonistic and antagonistic activity. Eur. J. Biochem. *267*, 3032–3039.

61. Rietschel, E.T., Kirikae, T., Schade, F.U., Mamat, U., Schmidt, G., Loppnow, H., Ulmer, A.J., Zähringer, U., Seydel, U., Di Padova, F., et al. (1994). Bacterial endotoxin: molecular relationships of structure to activity and function. FASEB J. *8*, 217–225.

62. Hamacher, K., Coenen, H.H., and Stöcklin, G. (1986). Efficient stereospecific synthesis of no-carrier-added 2-[18F]-fluoro-2-deoxy-D-glucose using aminopolyether supported nucleophilic substitution. J. Nucl. Med. *27*, 235–238.

63. Mannheim, J.G., Judenhofer, M.S., Schmid, A., Tillmanns, J., Stiller, D., Sossi, V., and Pichler, B.J. (2012). Quantification accuracy and partial volume effect in dependence of the attenuation correction of a state-of-the-art small animal PET scanner. Phys. Med. Biol. *57*, 3981–3993.

64. Lange, A., Beier, S., Steimle, A., Autenrieth, I.B., Huson, D.H., and Frick, J.S. (2016). Extensive Mobilome-Driven Genome Diversification in Mouse Gut-Associated Bacteroides vulgatus mpk. Genome Biol. Evol. *8*, 1197–1207.

65. Westphal, O., and Jann, K. (1965). Bacterial lipopolysaccharides: extraction with phenol-water and further applications of procedure. Carbohydr. Chem. *5*, 83–91.

66. Lutz, M.B., Kukutsch, N., Ogilvie, A.L., Rössner, S., Koch, F., Romani, N., and Schuler, G. (1999). An advanced culture method for generating large quantities of highly pure dendritic cells from mouse bone marrow. J. Immunol. Methods *223*, 77–92.

67. Jeon, S.G., Kayama, H., Ueda, Y., Takahashi, T., Asahara, T., Tsuji, H., Tsuji, N.M., Kiyono, H., Ma, J.S., Kusu, T., et al. (2012). Probiotic *Bifidobacterium breve* induces IL-10-producing Tr1 cells in the colon. PLoS Pathog. *8*, e1002714.

68. Rakoff-Nahoum, S., Paglino, J., Eslami-Varzaneh, F., Edberg, S., and Medzhitov, R. (2004). Recognition of commensal microflora by toll-like receptors is required for intestinal homeostasis. Cell *118*, 229–241.

69. Chow, J., and Mazmanian, S.K. (2010). A pathobiont of the microbiota balances host colonization and intestinal inflammation. Cell Host Microbe *7*, 265–276.

YMTHE, Volume *27*

Supplemental Information

Weak Agonistic LPS Restores Intestinal Immune Homeostasis

Alex Steimle, Lena Michaelis, Flaviana Di Lorenzo, Thorsten Kliem, Tobias Münzner, Jan Kevin Maerz, Andrea Schäfer, Anna Lange, Raphael Parusel, Kerstin Gronbach, Kerstin Fuchs, Alba Silipo, Hasan Halit Öz, Bernd J. Pichler, Ingo B. Autenrieth, Antonio Molinaro, and Julia-Stefanie Frick

Supplemental information

Supplemental information 1:

Comparison of surface molecule expression pattern of colonic lamina propria (cLP) CD11c+ cells and bone-marrow derived dendritic cells (BMDCs)

To verify the similarity of *ex vivo* isolated cLP CD11c+ cells with *in vitro* generated BMDCs in terms of expression of important surface markers, we stained both cell types with fluorophore-coupled antibodies for detection of CD11c, Ly6G, Ly6G, CD64, CD45R, CD45, CD103, CD11b and MHC-II (Figure S1). Viable cLP $CD11c^{+}$ single cells and viable BMDC single cells were demonstrated to provide similar expression of surface total MHC-II, CD45 and non-expression of Ly6G, Ly6C, CD64 and CD45R. We could detect slight differences in the expression of $CD103^{pos/neg}CD11b^{pos/neg}$ dendritic cell subpopulations, with BMDCs providing a slightly higher proportion of $CD103^{neg}CD11b^{pos}$ $CD11c^{+}$ cells while the $CD103^{neg}CD11b^{neg}$ subpopulation is slightly more frequent among cLP CD11c+ cells. However, these minor differences are assumed to be irrelevant for the performed experiments and conclusions.

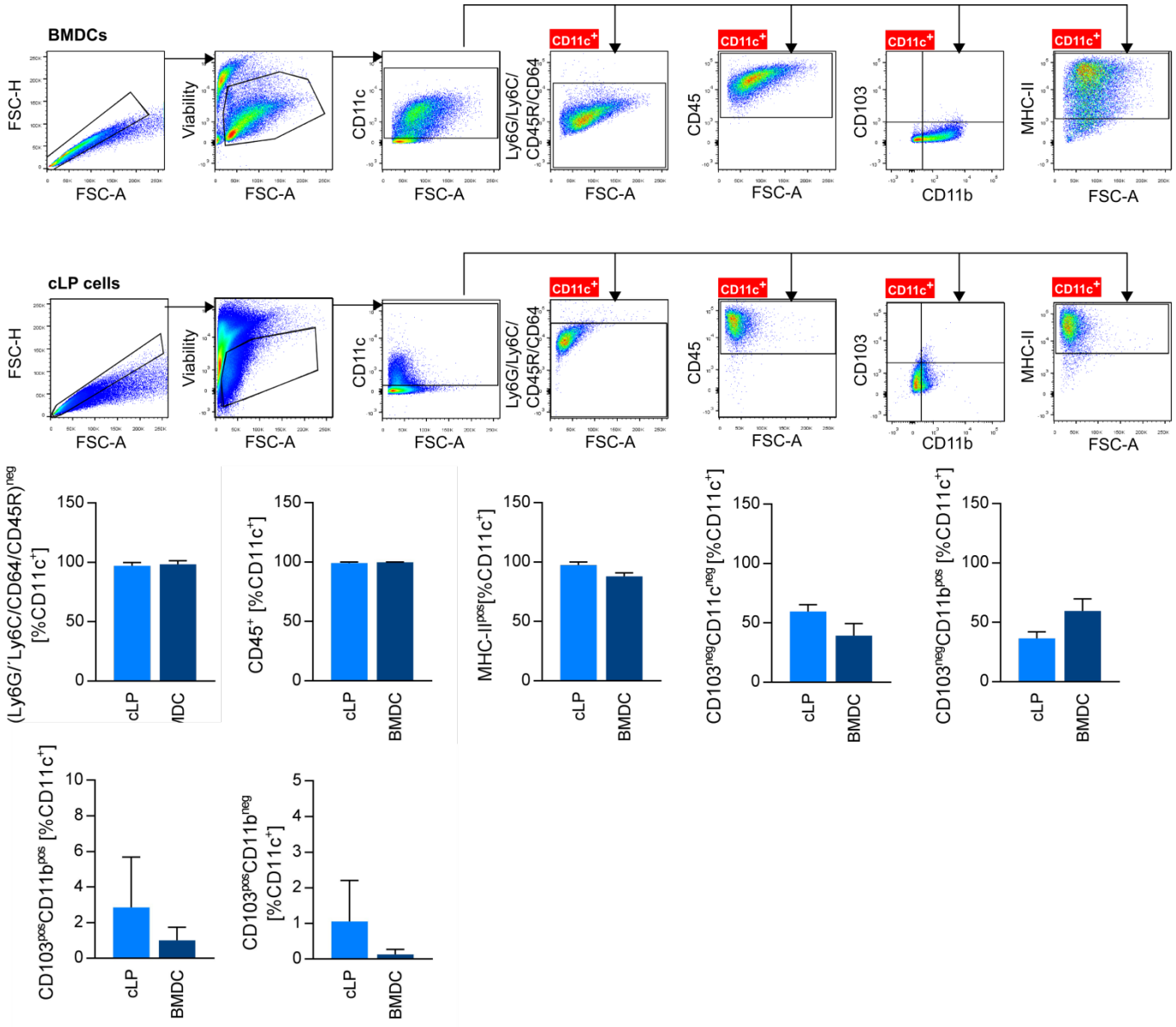

Figure S1: **Comparison between BMDCs and cLP CD11c+ cells.**

Bone-marrow derived dendritic cells (BMDCs) were generated as described in the Materials and Methods section. Colonic lamina propria (cLP) cells were isolated from $Rag1^{-/-}$ mice as described in the Materials and Methods section. Both cell types were stained with a fixable viability dye as well as with antibodies detecting CD11c, Ly6G, Ly6G, CD64, CD45R, CD45, CD103, CD11b and MHC-II. Upper panel and middle panel: Gating strategy for BMDCs (upper panel) and cLP cells (middle panel). Single cells

(FSC-A vs. FSC-H) were gated for viable cells. Viable single cells were gated for CD11c expression and $CD11c^+$ cells were analyzed for expression of Ly6G, Ly6C, CD64, CD45R, CD103, CD11b and MHC-II. Lower panel: Determination of surface expression of the respective surface molecules as a proportion of all $CD11c^+$ cells (n = 15 for each cell type). Columns and error bars represent mean ± SD

<u>Supplemental information 2</u>:

Gating strategy to determine CD40 surface expression as well as to define the subpopulation of MHC-II high positive cells

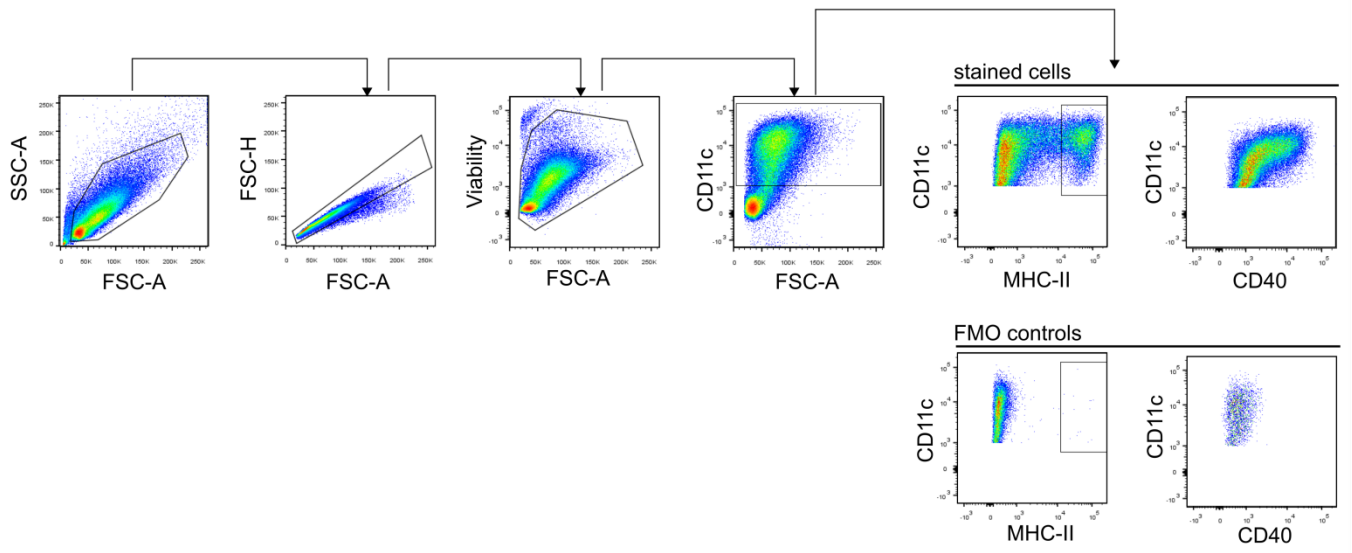

Figure S2: **BMDC gating strategy**

Gating strategy to determine CD40 surface expression as well as to define the subpopulation of MHC-II high positive cells. Viable, single $CD11c^{+}$ cells were stained for MHC-II and CD40 surface expression. Analysis of MHC-II surface expression was assessed by determination of the MHC-II high positive population, which is increased during DC maturation. CD40 expression was determined by measuring Median Fluorescence Intensity (MFI). The upper panel shows stained cells while the lower panel shows fluorescence-minus-one controls to determine $MHC\text{-}II^{neg}$ and $CD40^{neg}$ cells.

Supplemental information 3:

Heat-killed *Bacteroides* strains induce the same semi-mature phenotype in BMDCs as viable *Bacteroides* strains.

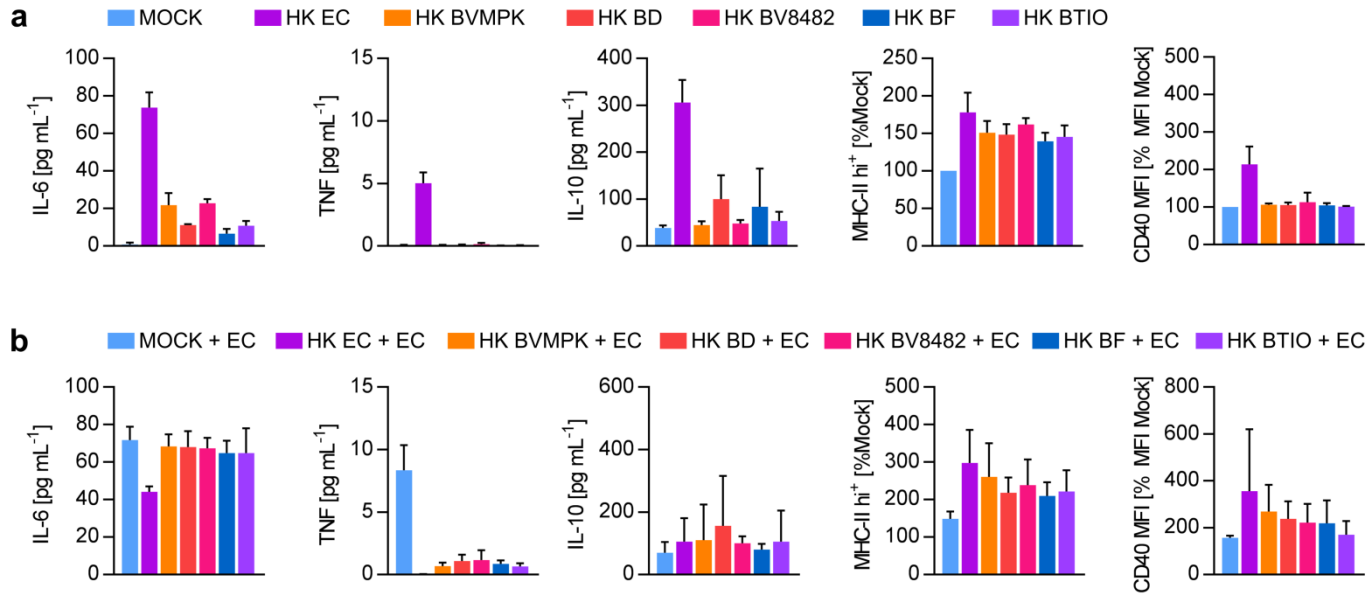

Figure S3: Heat-killed *Bacteroides* species induce the same hyporesponsive phenotype in CD11c+ cells as viable *Bacteroides* species

a) Stimulation of CD11c+ bone-marrow derived dendritic cells (BMDCs) generated from wt C57BL/6 mice (n=3) with PBS (Mock), heat-killed *E. coli* mpk (HK EC),heat-killed *B. vulgatus mpk* (HK BVMPK), heat-killed *B. dorei* (HK BD), heat-killed *B. vulgatus* ATCC8482 (HK BV8482), heat-killed *B. fragilis* (HK BF) and heat-killed *B. thetaiotaomicron* (HK BTIO) for 16 h at MOI 1. Cytokine secretion was detected by ELISA. Surface expression of MHC-II and CD40 was detected by flow cytometry and the population of MHC-II hi+ cells and CD40 MFI, respectively, was normalized to the mock control of BMDCs generated from the same individual. Columns and error bars represent mean ± SD.

b) *wt* BMDCs were stimulated with PBS (mock), HK EC, HK BVMPK, HK BD, HK BV482, HK BF and HK BTIO at MOI 1 for 24h (prime). Cell culture medium removed and exchanged for fresh medium before stimulation (challenge) with viable EC for additional 16 h. Cytokine secretion was detected by ELISA. Surface expression of MHC-II and CD40 was detected by flow cytometry and the population of MHC-II hi+ cells and CD40 MFI, respectively, was normalized to the mock-primed and EC-challenged control of BMDCs generated from the same individual. Columns and error bars represent mean ± SD.

Supplemental information 4:

Evaluation of TAK252 as a specific TLR4 inhibitor

To verify that TAK242 selectively inhibits TLR4 signalling, we treated BMDCs generated from wildtype mice with 10 µM TAK242 1h prior stimulation for 16 h with PBS (mock) LPS-EK as potent TLR4 ligand, FLA-ST as potent TLR5 ligand and PAM2CSK4 a potent TLR2 ligand, all at a final concentration of 100 ng/mL. Secretion of IL-6 as an indicator of TLR signalling was detected by ELISA. TAK242 significantly inhibited IL-6 secretion in cells stimulated with LPS-EK but showed no significant inhibitory activity in cells stimulated with FLA-ST or PAM2CSK4. This result supports findings by Lii *et al*., Takashima *et al.* and Matsunaga *et al* [1-3], observing no or only marginal binding of TAK242 to other TLRs compared to TLR4. We therefore consider TAK242 as a selective TLR4 inhibitor.

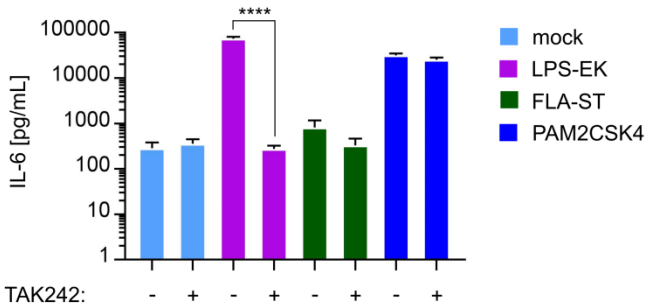

Figure S4:

TAK242 selectively inhibits TLR4 signaling

The competitive TLR4 antagonist TAK242 was added to CD11c+ bone-marrow derived dendritic cells (BMDCs) generated from wt C57BL/6 mice at a final concentration of 10 µM 1h prior to a stimulation for 16 h with with PBS (Mock) or ligands for TLR4 (LPS-EK, Invivogen), TLR5 (FLA-ST, Invivogen) and TLR2 (PAM2CSK4, Invivogen), all at a final concentration of 100 ng/mL. IL-6 secretion was detected by ELISA. Inhibitory activity of TAK242 is indicated by a significant reduction of IL-6 secretion in LPS stimulated cells but not in FLA-ST or PAM2CSK4-stimulated cells upon TAK242 treatment compared with mere TLR ligand stimulation. Columns and error bars represent mean ± SD.

Supplemental information 5:

Gating strategy to determine intracellular ALDH activity

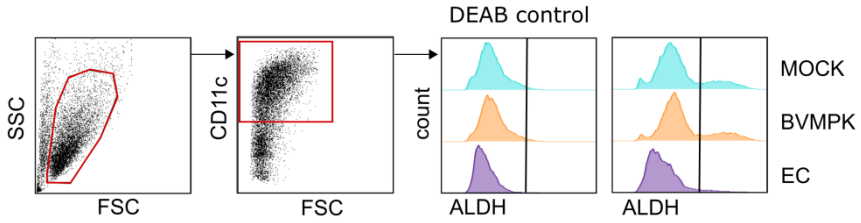

Figure S5: ALDH activity assay

Stimulation of $CD11c^+$ BMDCs generated from wt C57BL/6 mice with PBS (mock), *B. vulgatus* mpk (BVMPK) and *E. coli* mpk (EC) for 16 h. ALDH activity in stimulated cells was then analysed with the Aldefluor kit (Stemcell). Flow cytometric analysis with additional staining for CD11c was used to determine the mean fluorescence intensity (MFI) of $CD11c^+$ $ALDH^+$ cells. DEAB treated samples (left histogram panel) were used for determination of background fluorescence and defining $ALDH^+$cells , indicated by exemplary samples shown in right histogram panel.

Supplemental information 6:

LPSBV-induced semi-maturation of BMDCs requires TLR4, but not TLR2-signaling

We stimulated BMDCs generated from wildtype, TLR2-deficient, TLR4-deficient and TLR2xTLR4-double deficient mice with PBS (negative control), LPSBV (100 ng/mL) and EC (MOI1, positive control) and checked for subsequent secretion of pro-inflammatory cytokines IL-6 and TNF as well as surface expression of MHC-II and CD40. As already demonstrated in the main manuscript, stimulation of wildtype BMDCs with LPSBV resulted in intermediate secretion of IL-6, low to intermediate expression of MHC-II and CD40 as well as to absence of TNF compared to the EC positive control. IL-6 and TNF expression as well as increase in surface expression of MHC-II and CD40 was completely abolished using TLR4-deficient and TLR2xTLR4-double deficient BMDCs. Importantly, stimulation of TLR2-deficient BMDCs with LPSBV resulted in the same expression pattern of the detected cytokines and surface markers as LPSBV stimulation of wildtype BMDCs. To assess the contribution of a potential TLR2-signaling to the induction of LPSBV-induced semi-maturation in BMDCs, we primed TLR2-deficient BMDCs with PBS, LPSBV and EC and challenged them with either PBS or EC as a second stimulus as already demonstrated for wildtype BMDCs (Fig. 3). As shown in Figure S6b, hyporesponsiveness in terms of TNF and MHC-II expression was induced by LPSBV-priming, indicating that TLR2-mediated signaling is dispensable for LPSBV-induced BMDCs semi-maturation. Taken together, these results indicate that (1) either LPSBV or a potential contaminant induce a slight activation of TLR2-mediated signaling in mTLR2-HEK cells, (2) TLR4-signaling is far more important than TLR2-signaling for LPSBV-mediated effects on BMDCs in terms of cytokine expression and MHC-II/CD40 surface expression in response to stimulation with LPSBV preparations, (3) LPSBV or a potential contaminant does not activate TLR2 signaling in BMDCs and (4) LPSBV-induced MD-2/TLR4 receptor-signaling is essential for induction of semi-maturation in BMDCs.

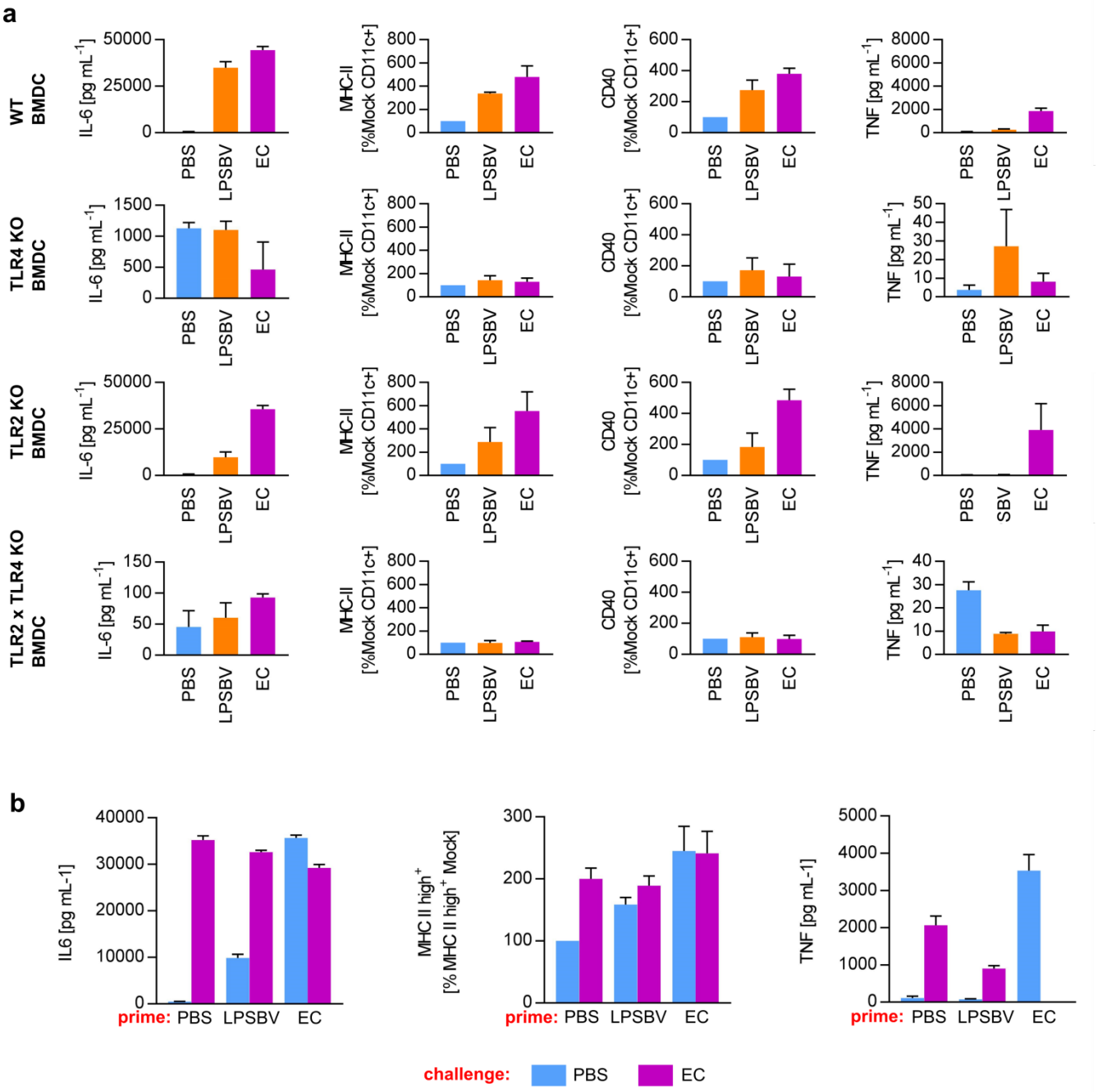

Figure S6: LPSBV-induced semi-maturation of BMDCs requires TLR4, but not TLR2-signaling

a) Stimulation of CD11c+ bone-marrow derived dendritic cells (BMDCs) generated from wt C57BL/6, TLR2-deficient, TLR4-deficient and TLR2xTLR4 double-deficient mice (n=4-8) with PBS (Mock), *E. coli* mpk (EC) and *B. vulgatus* mpk LPS (LPSBV). Cytokine secretion was detected by ELISA. Surface expression of MHC-II and CD40 was detected by flow cytometry and the population of MHC-II hi+ cells and CD40 MFI, respectively, was normalized to the mock control of BMDCs generated from the same individual. Columns and error bars represent mean ± SD.

b) TLR2-deficient BMDCs were stimulated with PBS (mock), EC or LPSBV for 24h (prime). Cell culture medium was removed and exchanged for fresh medium before stimulation (challenge) with EC or PBS for additional 16 h. Cytokine secretion was detected by ELISA. Surface expression of MHC-II and CD40 was detected by flow cytometry and the population of MHC-II hi+ cells and CD40 MFI, respectively, was normalized to the PBS-primed and PBS-challenged control of BMDCs generated from the same individual. Columns and error bars represent mean ± SD.

Supplemental information 7:

Biotinylation of LPSBV does not affect weak agonistic properties of LPSBV

To verify that biotinylation of LPSBV does not affect the weak agonistic properties of LPSBV, HEK cells overexpressing the mouse CD14/MD-2/TLR4-receptor complex were stimulated with LPSBV, bioLPSBV and LPSEC. We determined resulting expression of IL-8 as a measure of NFκB activation. We did not detect any differences in the NFκB activation in response to LPSBV compared to bioLPSBV (Figure 7)

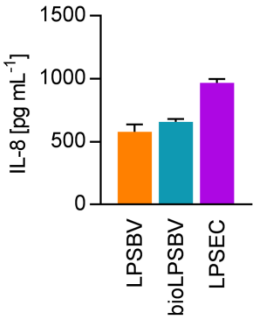

Figure S7: **Influence of LPSBV biotinylation on TLR4 receptor activation.**

mTLR4-HEK cells were stimulated with 10 ng/mL LPSBV, biotinylated LPSBV (bioLPSBV) and LPSEC. Resulting IL-8 concentration as a measure of intracellular NFκB activation was detected by ELISA. Columns and error bars represent mean ± SD.

Supplemental information 8:

Determination of quasi dissociation constants K_D of LPSBV and LPSEC

The observation that both LPS structures, LPS_{BV} and LPS_{EC}, showed different immunological effects on DCs *in vitro*, prompted us to define their binding affinity to the MD-2/TLR4 receptor complex. We established an experimental setting to determine *quasi* dissociation constants (K_D) of both LPS structures using biotinylated LPS_{BV} ($bioLPS_{BV}$). We are aware of the fact that we cannot determine real K_D-values since we do not know the exact molarity of the used LPS solutions. The assembly of amphiphilic LPS monomers into micelles, vesicles or even more complicated structures is highly dependent on the surrounding buffer and salt conditions and is therefore hardly predictable. This exacerbated the determination of the molarity of LPS monomers which effectively have access to the receptor, rendering them "active ligands" thus contributing to K_D values. However, assuming that (1) $bioLPS_{BV}$ and LPS_{EC} provide a comparable monomeric molecular weight, (2) $bioLPS_{BV}$ and LPS_{EC} behave in a similar chemical manner under the experimental conditions and (3) all experiments were carried out incubating both LPS at the same time, we can speculate that a qualitative comparison using K_D-values in the unit [g L^{-1}] instead of [mol L^{-1}] is qualifiable for a comparison of their binding affinity. In order to determine K_D values for both LPS structures, we used human embryonic kidney (HEK) cells which were stably transfected with a plasmid encoding for murine CD14, MD-2 and TLR4 (HEK-mTLR4). These latter were expressed by HEk-mTLR4 cells in excess and in equal amount by HEK-mTLR4 cells in all executed experiments, representing a fundamental prerequisite for K_D determination. LPS_{BV} was biotinylated ($bioLPS_{BV}$) as described in the experimental sections and its immunological behaviour was tested and compared to non-biotinylated LPS_{BV}. Since we could not detect any differences in the immunological behaviour (data not shown), we concluded that biotinylation did not affect the interaction with the receptor complex. We incubated HEK-mTLR4 cells with various concentrations of $bioLPS_{BV}$ and we then visualized bound $bioLPS_{BV}$ by adding PE-coupled streptavidin followed by flow cytometric analysis of the resulting PE fluorescence. As shown in Fig. S6a, non-biotinylated LPS and cells without addition of any LPS did not contribute to the PE fluorescence signal. The resulting PE-fluorescence in $bioLPS_{BV}$-treated samples was dependent on $bioLPS_{BV}$ concentration and showed a classical perpendicular hyperbola binding curve of a ligand to its respective receptor (Fig. S8a, right panel). In order to determine K_D of $bioLPS_{BV}$ and LPS_{EC} we simultaneously incubated HEK-mTLR4 cells with different concentrations of both LPS for 1 h and detected resulting PE fluorescence, which is directly proportional to the amount of bound $bioLPS_{BV}$ (Fig. S8b). In order to define the K_D value of $bioLPS_{BV}$, various concentrations of this LPS alone without addition of LPS_{EC} were used. The K_D equalled the concentration of $bioLPS_{BV}$ corresponding to the half maximal MFI PE intensity, which could be determined as 0.412 mg L^{-1}. In other words, adding 0.412 mg L^{-1} to the used 1 x 10^5 HEK-mTLR4 cells led to occupation of half of the available MD-2/TLR4 binding sites (Fig. S8c). In order to determine K_D of LPS_{EC}, several concentrations of LPS_{EC} were co-incubated with different concentrations of $bioLPS_{BV}$, resulting in 4 different binding curves representing the 4 employed LPS_{EC} concentrations (Fig. S8d). The resulting binding curves follow the equation

$$(1)\ MFI\ PE = \frac{n[bioLPS_{BV}]}{[bioLPS_{BV}] + K_D(bioLPS_{BV}) \times \left(1 + \frac{[LPS_{EC}]}{K_D(LPS_{EC})}\right)}$$

with n being the number of different binding sites (which was assumed to be 1 in our case). The binding curves shown in Fig. S8d were then plotted into a double reciprocal form resulting in 4 different straight lines whose slopes were determined using GraphPad Prism (Fig. S8e). The slopes obtained from Figure S8e were afterwards plotted against the respective LPS_{EC} concentration resulting in a straight line whose intersection with the x-axis represented the negative value of the LPS_{EC} binding constant which was determined to be 0.304 mg L^{-1}, being in the same biologically relevant range as $bioLPS_{BV}$ K_D. Therefore, based on the above described experiments, we can conclude that LPS_{BV} and LPS_{EC} provide similar binding affinity to the MD-2/TLR4 receptor complex.

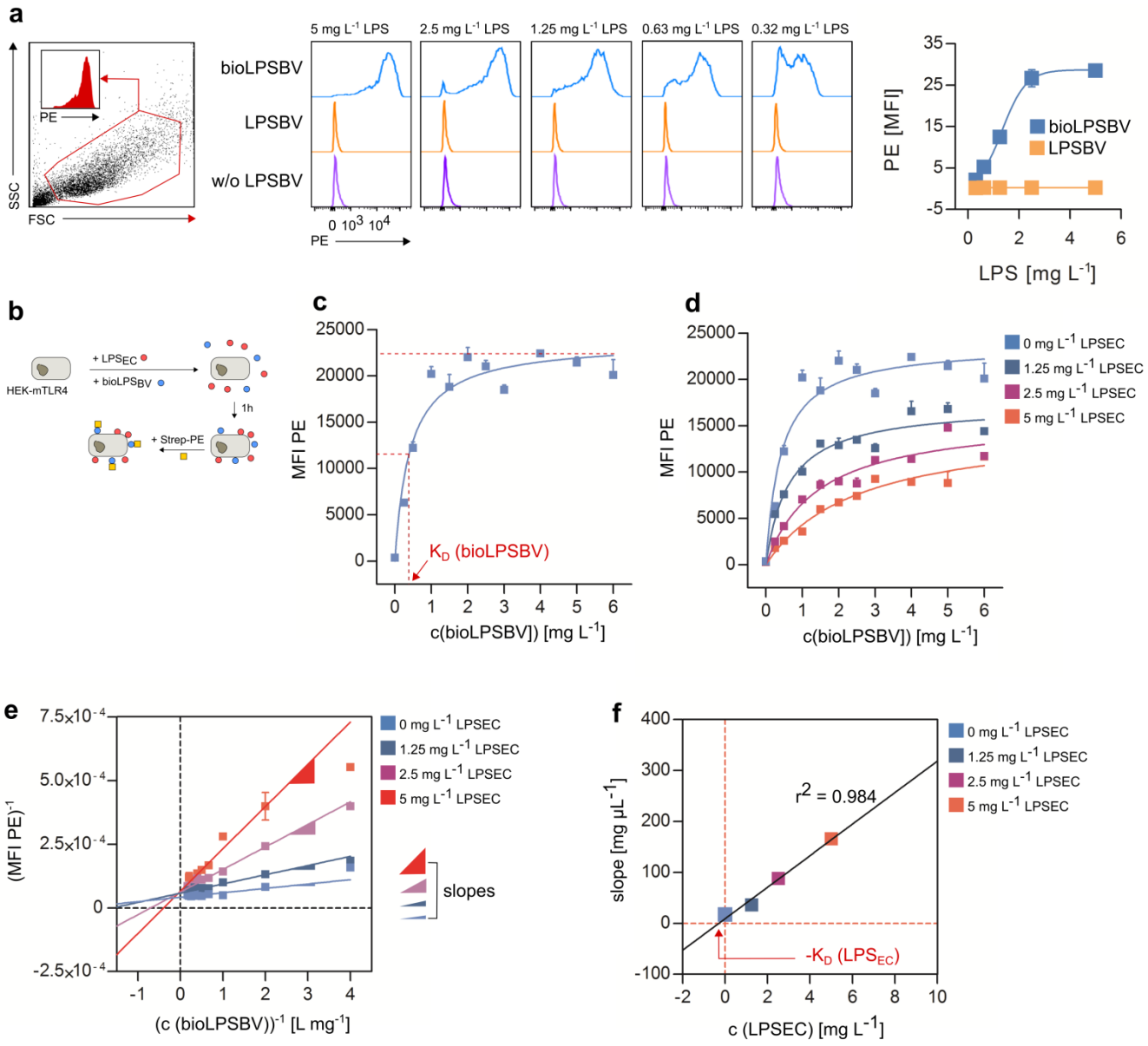

Figure S8: *B. vulgatus* mpk LPS and *E. coli* mpk LPS provide similar binding affinity to the MD-2/TLR4 receptor complex.

(a) Human embryonic kidney (HEK) cells expressing murine CD14, MD-2 and TLR4 (HEK-mTLR4) were co-incubated with *B. vulgatus* mpk LPS (LPSBV), biotinylated *B. vulgatus* mpk LPS (bioLPSBV) or PBS (w/o LPS_{BV}) at several concentrations. PE-coupled streptavidin (Strep-PE) was added to each sample in constant concentrations. Cells were washed and analysed afterwards for PE fluorescence using flow cytometry. Left panel: gating strategy to determine intact HEK-mTLR4 cells. Middle panel: representative histograms of PE fluorescence of intact HEK-mTLR4 cells that were treated as described above. Right panel: Detected mean PE fluorescence intensity (PE (MFI)) as a function of used $bioLPS_{BV}$ concentration.

(b) experimental setting for the determination of LPS binding affinity: HEK-mTLR4 cells were incubated simultaneously with various concentrations of non-biotinylated *E. coli* mpk LPS (LPSEC) or biotinylated *B. vulgatus* mpk LPS (bioLPSBV) for 1 h. Cells were washed and incubated with PE-coupled streptavidin (Strep-PE) for 30 min. PE fluorescence was detected afterwards using flow cytometry.

(c) HEK-mTLR4 cells were incubated with bioLPSBV only according to the experimental setting described in (b). By using different concentrations of bioLPSBV and the resulting detected PE fluorescence, a non-linear regression for a perpendicular hyperbola could be created. The bioLPSBV concentration corresponding to the half-maximal PE intensity equals to KD of bioLPSBV. Squares with error bars represent mean ± SD.

(d) according to (b) 1 x 10^5 HEK-mTLR4 cells were simultaneously incubated with bioLPSBV and LPSEC. For each differentially coloured perpendicular hyperbola binding curve the concentration of biotinylated *B. vulgatus* mpk LPS (bioLPSBV) was varied while the concentration of *E. coli* mpk LPS (LPSEC) was kept constant. According to (b), resulting PE fluorescence was detected by flow cytometry as demonstrated in (a). The detected PE signal is therefore directly proportional to bound bioLPSBV. Each data point represents a distinct combination of LPSEC and bioLPSBV concentrations (n=3). Squares with error bars represent mean ± SD.

(e) Data obtained from (d) were mathematically transformed into a double reciprocal form and plotted into a graph. The sigmoidal binding curves from (d) are therefore transformed into straight lines. The slopes of the straight lines were determined using GraphPad Prism. Squares with error bars represent mean ± SD.

(f) The slopes which were obtained from the double reciprocal plotting in (e) which were derived from the binding curves in (d) were plotted against the corresponding concentration of LPSEC which was kept constant in the experiment. A linearization led to a straight line whose intersection with the x-axis represents the negative value of the dissociation constant ($-K_D$) for the binding of LPS_{EC} to the murine MD-2/TLR4 receptor complex.

Supplemental information 9:

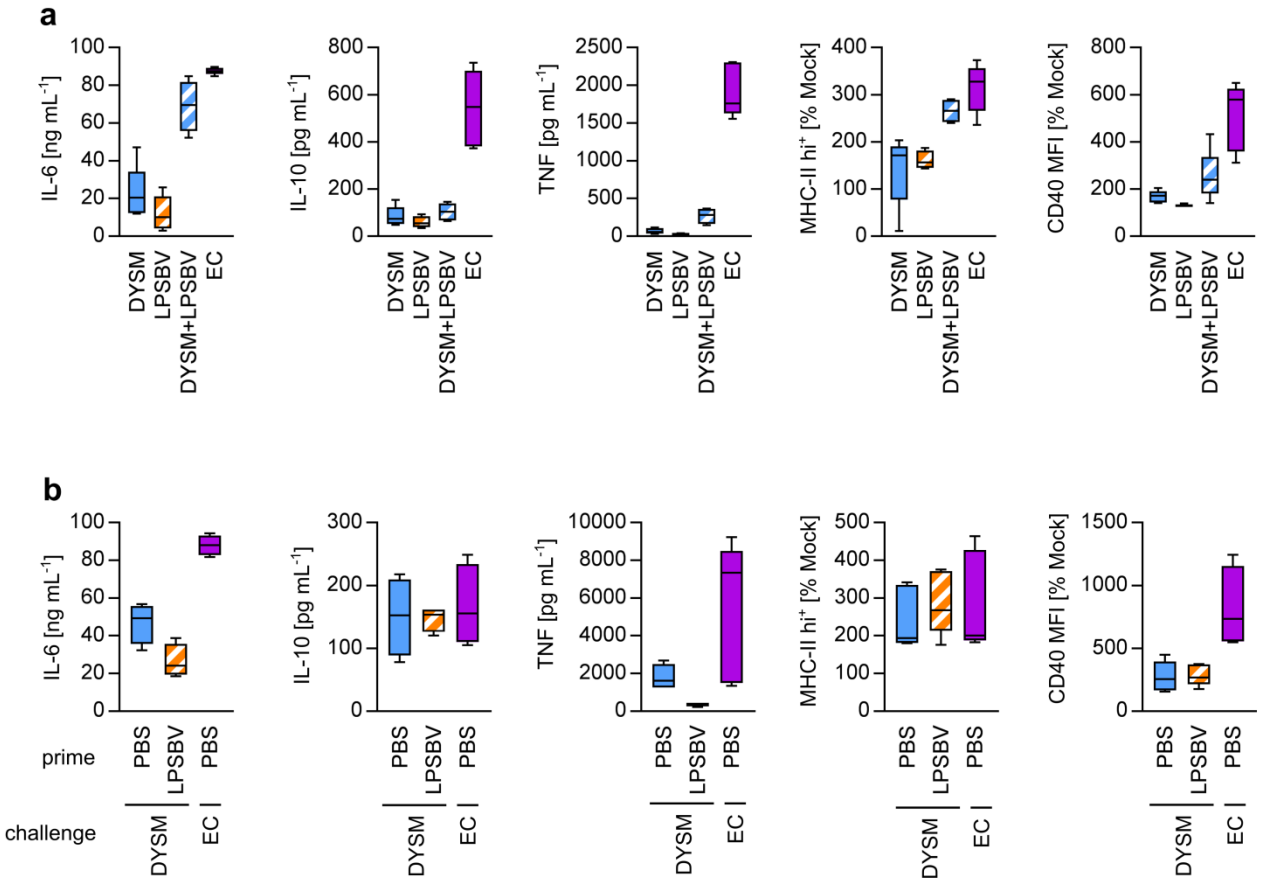

Figure S9:

a) Feces from *Rag1*$^{-/-}$ mice providing intestinal inflammation (DYSM) was autoclaved and prepared as described in Matherials and Methods. Wt BMDCs were stimulated with either DYSM, LPSBV (100 ng mL^{-1}), E. coli mpk (EC, MOI1)) or simultaneous (DYSM + LPSBV). Cytokine secretion was detected by ELISA. Surface expression of MHC-II and CD40 was detected by flow cytometry and normalized to the mock control of BMDCs generated from the same individual. Box plots depict the mean as well as the 25th and 75th percentile, whiskers depict the highest and lowest values.

b) wt BMDCs were stimulated (prime) with either PBS (mock) or LPSBV for 24 h. Medium was changed and cells were stimulated afterwards (challenge) with DYSM or EC (MOI 1). Cytokine secretion was detected by ELISA. Surface expression of MHC-II and CD40 was detected by flow cytometry and normalized to an unchallenged mock control of BMDCs generated from the same individual. Box plots depict the mean as well as the 25th and 75th percentile, whiskers depict the highest and lowest values.

Supplemental References:

1. Ii M, Matsunaga N, Hazeki K, et al. A novel cyclohexene derivative, ethyl (6R)-6-[N-(2-Chloro-4-fluorophenyl)sulfamoyl]cyclohex-1-ene-1-carboxylate (TAK-242), selectively inhibits toll-like receptor 4-mediated cytokine production through suppression of intracellular signaling. Mol Pharmacol 2006;69:1288-95.
2. Matsunaga N, Tsuchimori N, Matsumoto T, et al. TAK-242 (resatorvid), a small-molecule inhibitor of Toll-like receptor (TLR) 4 signaling, binds selectively to TLR4 and interferes with interactions between TLR4 and its adaptor molecules. Mol Pharmacol 2011;79:34-41.
3. Takashima K, Matsunaga N, Yoshimatsu M, et al. Analysis of binding site for the novel small-molecule TLR4 signal transduction inhibitor TAK-242 and its therapeutic effect on mouse sepsis model. Br J Pharmacol 2009;157:1250-62.